Multiple Scattered Radiation Emerging from Continental Haze Layers.

1: Radiance, Polarization, and Neutral Points

By

George W. Kattawar, Gilbert N. Plass, and Stephen J. Hitzfelder
Department of Physics
Texas A&M University
College Station, Texas 77843

Report No. 18

The research described in this report was

funded by the

National Aeronautics and Space Administration

Contract No. NGR 44-001-117

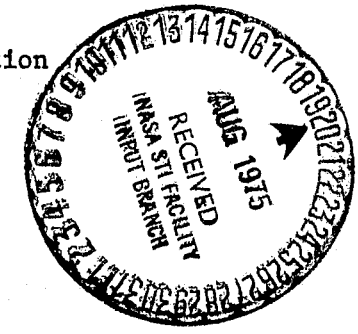

Department of Physics
Texas A&M University
College Station, Texas 77843

August 11, 1975

A paper based on the material in this report has been submitted to Applied Optics.

Multiple Scattered Radiation Emerging from Continental Haze Layers. 1: Radiance, Polarization, and Neutral Points

By George W. Kattawar, Gilbert N. Plass, and Stephen J. Hitzfelder

ABSTRACT

The complete radiation field including polarization is calculated by the matrix operator method for scattering layers of various optical thicknesses. Results obtained for Rayleigh scattering are compared with those for scattering from a continental haze. Radiances calculated using Stokes vectors show differences as large as 23% compared to the approximate scalar theory of radiative transfer, while the same differences are only of the order of 0.1% for a continental haze phase function. The polarization of the reflected and transmitted radiation is given for a wide range of optical thicknesses of the scattering layer, for various solar zenith angles, and various surface albedos. Two entirely different types of neutral points occur for aerosol phase functions. Rayleigh-like neutral points (RNP) arise from the zero polarization in single scattering that occurs for all phase functions at scattering angles of 0° and 180°. For Rayleigh phase functions, the position of the RNP varies appreciably with the optical thickness of the scattering layer. At low solar elevations there may be four RNP. For a continental haze phase function the position of the RNP in the reflected radiation shows only a small variation with the optical thickness, and the RNP exists in the transmitted radiation only for extremely small optical thicknesses. Another type of neutral point (NRNP) exists for aerosol phase functions. It is associated with the zeros of the single scattered polarization which occur between the end points of the curve; these are called non-Rayleigh neutral points (NRNP). There may be from zero to four of these neutral points associated with each zero

of the single scattering curve. They occur over a range of azimuthal angles, unlike the RNP which are in the principal plane only. The position of these neutral points is given as a function of solar angle and optical thickness.

The authors are with the Physics Department, Texas A&M University, College Station, Texas 77843.

I. Introduction

The radiation field produced by the photons which have undergone multiple scattering in a planetary atmosphere is in general polarized even though the incoming solar radiation is essentially unpolarized. Thus a complete description of the radiation scattered or transmitted by an atmospheric layer requires a specification of the degree and direction of polarization and the ellipticity in addition to the radiance.

Elegant and elaborate mathematical solutions have been developed for isotropic and Rayleigh scattering by Chandrasekhar,[1] Sekera,[2,3] Kourganoff,[4] and others. Numerical values for the various parameters of the diffuse radiation from a planetary atmosphere with Rayleigh scattering have been given in a set of tables published by Coulson et al.[5] These tables are limited to optical thicknesses of unity or less. Numerical results for Rayleigh scattering have also been presented by Herman and Browning,[6] Dave and Furukawa,[7] Kahle,[8,9] Howell and Jacobowitz,[10] Fymat and Abhyankar,[11] and Adams and Kattawar[12] among others. Among these authors only Dave and Furukawa[7] and Kahle[9] give radiance values for an optical thickness as large as 10. Most of the published results are for a surface albedo of zero. More recently Plass et al[13] have given radiance values out to large optical thicknesses and for a range of values of the surface albedo. Plass et al[14] have also calculated the radiance within optically deep absorbing media. Calculations of the polarization of the radiation are given only in Ref. 5, 6, 7, 10, and 11 and only Dave and Furukawa[7] give polarization values for an optical thickness as large as 10.

The radiation derived by scattering for a haze layer has been calculated by several different methods including Monte Carlo, iterative, doubling and matrix operator. Relatively few of these studies have included the

calculation of the polarization effects. Polarization values for the radiation scattered from various models of hazes have been reported by: Kattawar and Plass[15,18,20,21,23] and Plass and Kattawar[16,17,19,22] (Monte Carlo method) and by Dave,[24] Herman et al,[25] and Hansen[26] (iterative and doubling methods). Only Dave[24] has given results for the ellipticity and direction of polarization in addition to the radiance and polarization values, but only for a size parameter of 10 and up to an optical depth of 10. Hansen[26] gives the polarization of the reflected light only over a complete range of optical depths. The Monte Carlo results[15-23] cover a wide range of phase functions, optical depths, plane and spherical geometry, boundary surface including that of the ocean-atmosphere, but are averaged over a range of solid angle and necessarily have a certain statistical fluctuation in the results.

Matrix operator theory is an entirely rigorous and practical method for the solution of the equations of radiative transfer. A brief history of the method has been given by Plass et al.[13] Results calculated by this method include the radiance of the reflected and transmitted light for Rayleigh scattering layers[13] and for maritime haze[27] and the interior radiances in optically deep absorbing media scattering by the Rayleigh[14] and a continental haze[28] model.

The matrix operator method has been generalized so that all four components of the Stokes vector are calculated. From this the radiance, degree and direction of polarization, and the ellipticity of the scattered radiation is obtained. The results are presented in the two parts of this paper for scattering from Rayleigh and continental haze layers. The radiance calculated from the approximate scalar theory is compared with the results obtained from the complete Stokes vector for both Rayleigh and haze scattering. The neutral points where the polarization is zero are calculated for both of these types of scattering.

II. Computational Aspects

There is no difficulty in principle in generalizing the matrix operator method described by Plass *et al*[13] to calculate the complete radiation field. The radiance is replaced by the four component Stokes vector in all equations, while the phase function is replaced by the fourth order phase matrix. All of the equations are formally the same with these and other appropriate substitutions.

There are however, certain practical problems in the numerical solution of these equations. The storage requirements in the computer can become quite large and it is essential to minimize these as much as possible. These requirements can be greatly reduced by the use of the full symmetry relations which exist for the phase matrix of a spherical polydispersion as presented by Kattawar *et al*.[29]

The order of the quadrature used is determined by the accuracy with which the phase function can be normalized. The order of the quadrature is considered acceptable if the normalization of the phase function differs from unity by less than one part in 10^4. A symmetry preserving correction matrix is added so that normalization is achieved to the full accuracy of the computer. Great care was taken when adding the correction matrix. In extreme cases negative radiance values can be obtained even though the flux is conserved.[30]

A forty-second order Lobatto quadrature was used for the calculation presented in this article. Two different checks were made of these calculations against known results for scattering by the Rayleigh phase matrix. First the results for large optical depths were compared with the semi-infinite results given by Chandrasekhar[1]. The Stokes vectors computed from the formulae on page 261 of Chandrasekhar agree with our matrix operator results to one part in 10^4, which is the accuracy of the functions tabulated by Chandrasekhar. Second, careful comparisons were made with

the published tables of Coulson et al[5] for a wide range of the parameters. Excellent agreement (to one or two places in the last tabulated figure) was obtained for every element of the Stokes vector except in a few regions where there are obviously small errors in the Coulson tables. For example, the parameter Q for the transmitted radiation is given in the tables as -0.00034 when $\tau = 0.25$, $\mu_o = 1$, $\mu = 1$, when the correct value is exactly zero.

III. Radiance for Rayleigh Scattering---Approximate Scaler vs. Stokes Results

The upward radiance at the top of a plane parallel layer reflecting according to the Rayleigh phase matrix was calculated from the matrix operator theory and is shown in Fig. 1. The cosine of the solar zenith angle $\mu_o = 1$ and the surface albedo A = 0; the radiance is shown at various optical depths τ from 0.0019 to 4,096. These results are presented here mainly for later comparisons with those calculated for haze layers and from the approximate scalar theory. This figure shows a change from limb brightening to limb darkening as the optical depth of the scattering layer increases.

The diffuse downward radiance as observed at the bottom of the scattering layer is shown in Fig. 2 for $\mu_o = 1$. The maximum radiance is transmitted through such a scattering layer for optical thicknesses from about 1 to 4. The transmitted radiance becomes very small for the largest optical depth, $\tau = 1{,}024$, shown in the figure.

The accurate radiance values calculated from the complete theory using the four-component Stokes vector are compared with the approximate values obtained from the scalar radiative transfer theory which uses only a single equation involving the radiance. The fractional difference in these two results $\Delta R/R$ (R is exact radiance from Stokes vector; ΔR is the exact radiance minus the approximate scalar radiance) is shown in Fig. 3 for the reflected radiation when $\mu_o = 1$. The absolute value of the fractional difference between the two

results is small for small values of τ, increases to a maximum for τ around unity, and then decreases to a limiting value as τ increases further. The maximum absolute value of the fractional difference at $\tau = 1$ can be as large as 0.1 for a zenith angle of observation corresponding to $\mu = 0.15$. The maximum absolute value decreases to about 0.06 as τ becomes large.

The fractional difference in these two results is shown in Fig. 4 for the radiation transmitted through a layer of optical thickness τ. The absolute value of $\Delta R/R$ is a maximum for optical thicknesses around unity and then starts to decrease rapidly as τ increases further and is quite small for $\tau \geq 16$. The largest difference that we found is when the sun is near the horizon and the observer is looking close to the horizon, when $\mu_o = 0.03785$, $\mu = 0.03785$, $\tau = 1$, $\phi = 0^o$, the exact radiance is 0.001625, while the scalar theory gives 0.001998, for a difference of 23.0%.

Radiance values calculated from the approximate scalar theory of radiative transfer for Rayleigh scattering can be in error by up to 23% at optical thicknesses around unity and for the reflected radiation may be in error by 6 to 10% for all $\tau \geq 1$. Whether an error of this size is significant in a particular problem can only be determined by the proposed use of the results.

IV. Radiance for Haze L---Approximate Scaler vs. Stokes results

Calculations were made of the complete radiation field scattered from the top of and transmitted through the bottom of a plane parallel continental haze layer. The haze L model proposed by Deirmendjian[31] is used. The number of particles with a given radius is proportional to $r^2 \exp(-15.1186r^{1/2})$, where r is the particle radius. The mode radius is 0.07 μm. A wavelength of $\lambda = 0.55$ μm and real and imaginary parts of the index of refraction $n_1 = 1.55$ and $n_2 = 0.05$ were assumed as a reasonable approximation to the appropriate values for real continental hazes. The single scattering phase matrix was calculated by the method described by Kattawar and Plass[32] and Kattawar et al[29]. The Mie scat-

tering matrix was obtained for size parameters $x = 2\pi r/\lambda$ from 0.05 to 30 using a 75th order Gauss quadrature. The calculated single scattering albedo is 0.7171. The single scattering function obtained from this phase matrix is shown in Fig. 5. There is a fairly strong maximum in the backward direction and a slight maximum at the rainbow angle.

The upward radiance reflected from the top of a plane parallel haze L layer of optical thickness τ is shown in Fig. 6 for $\mu_o = 0.85332$ and $A = 0$. The azimuthal angle ϕ is measured from the incident plane that contains the incident ray and the zenith direction. Here $\phi = 0^o$ on the left half of the figure and $\phi = 180^o$ on the right half; the antisolar point occurs in the right half of the figure. Thus as μ varies from the left to the right in Fig. 6, we obtain the radiance values from the solar horizon to the nadir and then back through the antisolar point to the antisolar horizon. In all cases in this article the incoming solar flux is normalized to unity in a direction perpendicular to the solar beam. A maximum in the curve for the reflected radiance can be observed in Fig. 6 for all optical thicknesses near $\mu = 0.853$ and $\phi = 180^o$. This is caused by the glory, the maximum in the single scattering curve for 180^o scattering. The curve shown for $\tau = 16$ is a limiting curve which does not change further on the scale of the graph for larger optical thicknesses.

The diffuse downward radiance transmitted through the bottom of a haze L layer of optical thickness τ is shown in Fig. 7 for $\mu_o = 0.85332$ (31.43^o) and $A = 0$. As τ varies from the left to the right in Fig. 7, we obtain the radiance values from the solar horizon through the solar point to the zenith and then back to the antisolar horizon. At very small optical thicknesses there is the expected maximum around the solar direction from the strong forward scattering of the phase function in addition to maxima at each horizon. As the optical thickness of the layer increases, the maximum around the solar direction noticably decreases and shifts toward the zenith when τ is as large as 8. When $\tau = 16$, the radiance has a maximum at the zenith and no longer shows any

variation with azimuthal angle on the scale of this graph.

In order to study the variation of the radiance with solar angle, the upward and downward radiance for $\mu_o = 0.13817$ (79.15^o) is shown in Figs. 8 and 9. The upward radiance for small optical thicknesses varies by four orders of magnitude between the solar horizon and the nadir and increases by two orders of magnitude from the nadir to the antisolar horizon.

The downward radiance shown in Fig. 9 is particularly interesting as it illustrates how the position of maximum radiance moves from the horizon to the zenith as the optical thickness of the haze layer increases. When $\tau = 0.00195$ and 0.0625, the maximum is at the solar horizon. For larger optical thicknesses of the layer the angles at which the maximum radiance occurs is given in Table I for solar zenith angles of 31.43^o and 79.15^o.

In the previous section it was shown that there may be differences as large as 23% in the radiance calculated from the approximate scalar theory compared to the correct value for the Rayleigh phase matrix. Are these differences as large for other types of phase functions? The haze L model was used for the calculation of the radiance by both the approximate scalar theory and by the correct Stokes vector theory. The results are compared in Table II. A comparison of a large number of these results for different values of τ, μ_o, and ϕ showed extremely good agreement between the radiance results from these two theories. The largest differences found were of the order of 0.1%. The differences are much smaller than is the case for Rayleigh scattering, because of the smaller size of the off-diagonal matrix elements for the haze than for Rayleigh scattering.

V. Polarization for Rayleigh Scattering

In order to understand and appreciate the complexity of the polarization curves for haze L, it is necessary to study first the results for Rayleigh scattering. A few such results are given in this section.

The polarization of the photons reflected from a Rayleigh layer is shown in Fig. 10 for $\mu_o = 0.18817$ (79.15^o), A = 0, and $\phi = 0^o$. The polarization of single scattered photons from a Rayleigh scattering function is well known to be zero for scattering angles of 0^o and 180^o and to be a maximum at 90^o. The curve for $\tau = 0$ in Fig. 10 refers to single scattered photons and is zero when $\mu = 0.18817$ ($\theta = 79.15^o$, the antisolar direction; scattering angle = 180^o and is unity when $\mu = 0.98214$ ($\theta = 10.85^o$; scattering angle = 90^o). As soon as there is a finite optical thickness, the single neutral point at the antisolar direction splits into two neutral points, one on each side. As the optical thickness, increases the neutral points move farther away from the original position. One neutral point eventually reaches the antisolar horizon and then reappears just above the solar horizon. The polarization of the reflected radiation in general decreases as τ increases in regions away from the neutral points (a broad region around the nadir in the example shown in Fig. 10), but may increase appreciably as τ increases in a region around the antisolar direction. The curve shown for $\tau = 4$ is a limiting curve that does not change on the scale of this figure as τ increases further.

The neutral points that develop for Rayleigh scattering have often been discussed in the literature. The most complete curves previously published showing the position of the neutral points as a function of the optical thickness of the layer are those of Dave and Furukawa[7]. However, their curves are for the transmitted radiation only and for a single solar zenith angle (84.26^o). They pointed out for the first time that there are four neutral points over a certain range of optical thickness near unity at this particular solar zenith angle.

The neutral points for the reflected radiation as a function of the optical thickness of the reflecting layer are shown in Fig. 11 for $\mu_o = 0.85332$ (31.43^o), $\mu_o = 0.11333$ (83.49^o), and $\mu_o = 0.03785$ (87.83^o). The ordinate of these figures is the cosine of the nadir angle of observation and the abscissa is the optical

thickness of the reflecting layer. The Babinet point (between the antisolar direction and the nadir) moves toward the nadir as the optical thickness increases. It reaches a limiting position at an optical thickness of about 10 that does not change further as the optical thickness further increases. Curves are shown for several surface albedos (A = 0 and 1). The position of the Babinet point is relatively insensitive to A.

The Brewster point (between the antisolar direction and the antisolar horizon) moves from the antisolar point toward the antisolar horizon as the optical thickness increases. When the sun is sufficiently near the horizon, the Brewster point touches the antisolar horizon at some value of the optical thickness. As the optical thickness further increases, the neutral point reappears on the solar horizon and is now called the Arago point (between the solar horizon and the nadir). A further increase in the optical thickness causes the Arago point to move up from the solar horizon. The position of the Brewster and Arago points depends slightly on the surface albedo A. When the position of the Brewster and Arago points is plotted as in Fig. 11, the curve is continuous across the horizon.

The position of the neutral points when $\mu_o = 0.53786$ (57.46^o) and $\mu_o = 0.18817$ (79.15^o) is given in Fig. 12. The position of the Brewster point for $\theta_o = 57.46^o$ is relatively sensitive to the surface albedo A.

The polarization of the transmitted photons for $\mu_o = 0.18817$ (79.15^o), A = 0, and $\phi = 0^o$ and 180^o is given in Fig. 13. In this case the single scattered photons have zero polari ation when $\mu = 0.18817$ ($\theta = 79.15^o$, the solar direction; scattering angle = 0^o). As the optical thickness of the layer increases, the two neutral points move out from $\mu = 0.18817$. Eventually one neutral point appears on the antisolar horizon. When $1 < \tau < 2.5$, there are four neutral points, and, when $\tau > 2.5$, there are none. The polarization curve for $\tau = 4$ has no zeros and has relative maxima near the zenith and at both horizons. This curve is not quite symmetric around the zenith.

The shape of the polarization curve for radiation transmitted through a layer of optical thickness τ is entirely different when $\tau = 16$. This is an asymptotic curve which is the same for all layers with larger optical thicknesses. The polarization is zero at the zenith. After the photon has passed through the diffusion region in the scattering layer, it has lost all memory of its original direction; thus the polarization at the zenith of the radiation leaving the lower surface of the medium must be zero, since there can be no preferred direction. Furthermore the curve must be independent of the azimuthal angle. It is perhaps somewhat surprising that the radiation emerging near the horizon from a very thick Rayleigh scattering layer has a polarization of the order of 10%.

The position of the neutral points of the radiation transmitted through a Rayleigh layer of given optical thickness is shown in Figs. 14 - 17 for four different solar angles. The position of the neutral points when $\mu_o = 0.85332$ (31.43^o) is given in Fig. 14, a case typical of those with the sun near the zenith. The Babinet point (between the solar direction and the zenith) moves from the solar direction toward the zenith as the optical thickness increases, reaches a maximum displacement at about $\tau = 1.3$, and then moves back toward the solar direction to meet the Brewster point at $\tau = 5.2$. There are no neutral points at larger values of τ when $A = 0$. The Brewster point (between the solar direction and the solar horizon) moves from the solar direction toward the solar horizon as τ increases, reaches a maximum displacement at about $\tau = 2.1$, and then moves back toward the solar direction to meet the Babinet point. There is a considerable difference in the curves for a surface albedo $A = 0$ and $A = 1$, but little difference between $A = 0$ and $A = 0.2$. There are never more than two neutral points for this solar angle.

The same curves, but for $\mu_o = 0.53786$ (57.46^o) are given in Fig. 15. The unusual aspect of this example is that only Babinet and Brewster points exist when the surface albedo $A = 0$, while an Arago point (between antisolar horizon and zenith) exists when $0.68 < \tau > 3.4$ and $A = 1$.

The neutral points when $\mu_o = 0.18817$ (79.15^o) are shown in Fig. 16. When the sun is this close to the horizon an interesting new phenomenon appears (as was pointed out for the case $\mu_o = 0.1$ by Dave and Furukawa[7]). Four neutral points (two Arago, one Brewster, and one Babinet) appear over the range of optical thickness from 1.2 to 1.8 when A = 0. There is another range of optical thickness from about 2.0 to 2.5 where there are two Babinet points and no others.

The curves when $\mu_o = 0.03785$ (87.83^o) are given in Fig. 17. There is one Babinet and one Brewster point for A = 0 when $\tau < 0.0015$; one Babinet and one Arago point when $0.0015 < \tau < 0.96$; one Babinet, one Brewster, and two Arago points when $0.96 < \tau < 1.1$; two Babinet and two Arago points when $1.1 < \tau < 1.6$; two Babinet points when $1.6 < \tau < 1.7$; no neutral points when $\tau > 1.7$.

VI. Polarization for Haze L Scattering

The polarization of the radiation scattered by aerosol layers exhibits various new features which are not found in scattering from Rayleigh type particles. One major difference is that the polarization of single scattered radiation from Rayleigh particles is zero only at the end points (scattering angle $\phi = 0^o$ and 180^o). In general, when there is moderate or no absorption, the single scattered polarization of radiation scattered from aerosols exhibits one or more zeros in between the end points of the curve.

The polarization of single scattered photons from haze L is shown in Fig. 18 as a function of the cosine of the scattering angle Θ. Four different curves show the polarization on succesively magnified scales. The following points should be noted: 1. the polarization reaches a maximum value of about 0.53 at $\Theta \sim 158^o$; 2. the polarization is zero for scattering angles of 3.53^o and 25.6^o; 3. the polarization is very small (less than 10^{-5}) for $0^o < \Theta < 3.53^o$; 4. the absolute value of the polarization is small (less than 0.0064) for $3.53^o < \Theta < 25.6^o$.

The single scattered photons have zero polarization whenever the scattering angle in three dimensions is either 3.53° or 25.6°. There are two curves for each solar zenith angle in Fig. 19, which give the corresponding polar coordinates of these particular scattering angles. Any point on a curve gives a value for μ (cosine of the zenith angle) and of ϕ (azimuthal angle) for which the polarization is zero. There are two curves for each solar zenith angle; the small curve near the left hand edge of the figure is for the scattering angle 3.53°, while the other curve is for 25.6°. When the sun is near the zenith the polarization can be zero for $\Theta = 3.53^{\circ}$ and 25.6° only for the radiation transmitted through the bottom of the layer, but not for the reflected radiation; on the other hand, when the sun is close to the horizon, there are in addition angles at which the polarization is zero for the radiation reflected from the top of the layer.

These neutral points will be called NRNP (non-Rayleigh neutral points), since they have no counterpart in Rayleigh scattering. The NRNP arise from zeros in the single scattering polarization curve at scattering angles between 0° and 180°. On the other hand the RNP (Rayleigh neutral points) arise from the zeros that always occur in the single scattering polarization curve at the end points ($\Theta = 0^{\circ}$ and 180°). As our examples will show, the behavior of the polarization near NRNP and RNP is quite different as the optical thickness increases.

The polarization of the radiation reflected from and transmitted through haze L layers is shown in the following examples. The polarization of the reflected photons is given in Fig. 20 when $\mu_o = 0.85332$ (31.43°). The curves in the upper part of the figure are for the principal plane ($\phi = 0^{\circ}$ and 180°), while those in the lower part are for $\phi = 30^{\circ}$ and 150°. For single scattering ($\tau \doteq 0$) there is only a RNP in the principal plane when $\mu_o = 0.85332$. There is no NRNP for the reflected radiation at such a high sun angle. As τ increases two neutral points develop around the single scattering RNP, just as occurs for scattering from Rayleigh type particles. In the present case the two neutral

points never move as far from $\mu_o = 0.85332$ as they do in the case of Rayleigh scattering. They move less than 3^o as is shown in Table III.

The largest values of the polarization in Fig. 20 occur in two regions on either side of the RNP near angles of observation that correspond to a single scattering angle of 158^o from the incident solar beam.

The position of the RNP as a function of the optical thickness of the reflecting haze L layer is shown in Fig. 21 for five different solar zenith angles. In all cases there is a relatively small change (usually less than 5^o) in the position of the RNP as the optical thickness increases from zero. The small variation in these neutral points is in sharp contrast to the much larger changes that occur for scattering from a Rayleigh phase function.

The polarization of the reflected photons for $\mu_o = 0.85332$ in the plane at right angles to the principal plane ($\phi = 90^o$) is given in the top part of Fig. 22 (with the polarization of the photons transmitted through the layer in the lower part of the figure).

An example of the polarization of the reflected photons from a haze L layer when the sun is near the horizon is given in Fig. 23 for the case $\mu_o = 0.188166$ (79.15^o). The RNP exist near the antisolar direction ($\mu = 0.188166$, $\phi = 180^o$). As the optical thickness increases these move away from the antisolar direction as shown in Fig. 21 and in Table III. In addition, at this low solar angle, there is also a single NRNP near $\mu = 0.26$ (75.2^o; $\phi = 0^o$). As previously discussed and shown in Fig. 19, the scattering angle for the single scattered reflected photons is 25.6^o in this direction; this scattering angle corresponds to a zero in the single scattering function for haze L and causes this NRNP. The position of this NRNP changes only slightly as the optical thickness of the reflecting layer increases; Table III shows that it changes from 75.2^o for $\tau = 0$ to 75.9^o for a large optical thickness.

The polarization of the photons transmitted through a haze L layer is shown in Fig. 24 when $\mu_o = 0.85332$ (31.43^o) and $\phi = 0^o$ and 180^o. First there is a RNP at $\mu = 0.85332$, $\phi = 0^o$ for single scattered photons ($\tau = 0$). This RNP no longer exists for radiation transmitted through layers of even very small optical thickness, presumably because of the extremely small values for the single scattered polarization at small scattering angles.

In addition there are two NRNP which are near $\mu = 0.544$ (57.0^o) and 0.9952 (5.6^o). As the optical thickness increases, these NRNP change their position as indicated in Fig. 24 and Table III. They finally disappear for an optical thickness between 8 and 16.

The polarization curves for the plane $\phi = 30^o$ and 150^o are shown in Fig. 25. For small optical thicknesses there are two NRNP near $\mu = 0.66$ and 0.99 at the angles indicated in Fig. 19. The position of one of these NRNP changes appreciably when $\tau = 4$ and both NRNP disappear for an optical thickness between 4 and 8. The NRNP occur over a range of azimuthal angles, while the RNP never occur outside of the principal plane.

The nature of the polarization curves is quite different at low solar elevations as shown in Fig. 26 for the case $\mu_o = 0.188166$. There is a RNP at $\mu = 0.188166$ and $\phi = 0^o$ for single scattered photons; it disappears for layers with very small optical thicknesses. There is one NRNP at $\mu = 0.593$ (53.6^o) for single scattered photons, the position indicated in Fig. 19. As the optical thickness of the haze layer increases, this NRNP has moved only slightly to 57.6^o for $\tau = 2$ (see Fig. 26 and Table III). Interestingly a second neutral point appears at the horizon when $\tau = 1.4$ and there are two NRNP when $1.4 < \tau < 2.3$. When $\tau = 2$ the two NRNP are at 57.6^o and 70.1^o (see Fig. 26 and Table III). There are no neutral points for the transmitted radiation when $\tau > 2.3$.

The position of the NRNP for five solar angles is given in Fig. 27. The curves vary greatly in shape depending on the solar angle. There are one or two NRNP depending on the optical thickness. There is a suggestion in the curve for

$\mu = 0.53786$ that four NRNP exist over a very narrow range of optical thickness.

VII. Conclusions

The polarization of the radiation reflected from and transmitted through a scattering layer is compared for Rayleigh and haze L phase matrices. In both cases there are neutral points arising from the zeros of the polarization of single scattered photons at scattering angles of 0° and 180°. The angular position of these Rayleigh-like neutral points (RNP) in the sky shows appreciable variation with the optical thickness of the scattering layer for a Rayleigh phase matrix, but only a small variation for haze L. In fact RNP exist for the transmitted radiation through a haze L layer only when the optical thickness is extremely small. RNP exist only in the principal plane.

Another type of neutral point exists for non-Rayleigh phase functions which is associated with the zeros of the polarization for single scattering which occur between the end points of the curve; these are called non-Rayleigh neutral points. For a given optical thickness there may be zero, one, two, or even four of these neutral points associated with each of the zeros of the polarization for single scattering. NRNP occur over a range of azimuthal angles starting from the principal plane.

A comparison of radiances calculated from the complete theory of radiative transfer using Stokes vectors with those obtained from the scalar theory shows that differences of the order of 23% may be obtained for Rayleigh scattering, while the largest difference found for a haze L phase function was of the order of 0.1%. The scalar theory can apparently be used with confidence to calculate radiances for hazes and aerosols.

This work was supported in part by Grant No. NGR 44-001-117 from the National Aeronautics and Space Administration. Acknowledgement is made to the National Center for Atmospheric Research, which is sponsored by the National Science Foundation, for computer time used in this research.

References

1. S. Chandrasekhar, Radiative Transfer (Oxford U. P., New York, 1950).

2. Z. Sekera, Adv. Geophys, 3, 43 (1956).

3. Z. Sekera, "Polarization of Skylight," in Handbuch der Physik, S. Flugge, Ed. (Springer, Berlin, 1957), Vol. 48, p. 288-328.

4. V. Kourganoff, Basic Methods in Transfer Problems (Clarendon, Oxford, 1952).

5. K. L. Coulson, J. V. Dave, and Z. Sekera, Tables Related to Radiation Emerging from a Planetary Atmosphere with Rayleigh Scattering (University of California Press, Los Angeles, 1960).

6. B. M. Herman, and S. R. Browning, J. Atmos. Sci. 22, 559 (1970).

7. J. V. Dave, and P. M. Furukawa, J. Opt. Soc. Am. 56, 394 (1966).

8. A. B. Kahle, J. Geophy. Res. 73, 7511 (1968).

9. A. B. Kahle, Astrophy. J. 151, 637 (1968).

10. H. B. Howell, and H. Jacobowitz, J. Atmos. Sci. 27, 1195 (1970).

11. A. L. Fymat, and K. D. Abhyankar, J. Geophy. Res. 76, 732 (1971).

12. C. N. Adams, and G. W. Kattawar, J. Quant. Spectrosc. Radiat. Transfer 10, 341 (1970).

13. G. N. Plass, G. W. Kattawar, and F. E. Catchings, App. Opt. 12, 314 (1973).

14. G. N. Plass, G. W. Kattawar, and J. Binstock, J. Quant. Spectrosc. Radiat. Transfer 13, 1081 (1973).

15. G. W. Kattawar, and G. N. Plass, Appl. Opt. 7, 1519 (1968).

16. G. N. Plass, and G. W. Kattawar, Appl. Opt. 8, 2489 (1969).

17. G. N. Plass, and G. W. Kattawar, Appl. Opt. 9, 1122 (1970).

18. G. W. Kattawar, and G. N. Plass, Appl. Opt. 10, 74 (1971).

19. G. N. Plass, and G. W. Kattawar, J. Atmospheric Sci. 28, 1187 (1971).

20. G. W. Kattawar, G. N. Plass, and C. N. Adams, Astrophy. J. 170, 371 (1971).

21. G. W. Kattawar, and G. N. Plass, Appl. Opt. 11, 2851 (1972).

22. G. N. Plass, and G. W. Kattawar, Appl. Opt. 11, 2866 (1972).

23. G. W. Kattawar, G. N. Plass, and J. A. Guinn, Jr., J. Phys. Oceanography 3, 353 (1973).

24. J. V. Dave, Appl. Opt. 9, 2673 (1970).

25. B. M. Herman, S. R. Browning, and R. J. Curran, J. Atmos. Sci. 28 419 (1971).

26. J. E. Hansen, J. Atmos. Sci. 28, 1400 (1971).

27. G. W. Kattawar, G. N. Plass, and F. E. Catchings, Appl. Opt. 12 1071 (1973). The mode radius given on p. 1071 should be changed to 0.05.

28. G. W. Kattawar, and G. N. Plass, J. Quant. Spectrosc. Radiat. Transfer 15, 61 (1975).

29. G. W. Kattawar, S. J. Hitzfelder, and J. Binstock, J. Atmos. Sci. 30, 289 (1973).

30. G. W. Kattawar, J. Quant. Spectrosc. Radiat. Transfer 13, 145 (1973).

31. D. Deirmendjian, Electromagnetic Scattering on Spherical Polydispersions (American Elsevier, New York, 1969).

32. G. W. Kattawar and G. N. Plass, Appl. Opt. 6, 1377 (1967).

Table I.

Angles for maximum radiance and polarization.

Solar Zenith Angle	Optical thickness	Zenith angle for maximum downward radiance ($\phi=0^{o}$)	Maximum Polarization of downward radiance ($\phi=180^{o}$)	Maximum Polarization of upward radiance ($\phi=180^{o}$)	
			Zenith Angle	Nadir angle	Nadir angle
31.43^{o}	0			53.56^{o}	10.36^{o}
	0.00195	32.22^{o}		53.56^{o}	10.36^{o}
	0.00781	32.22^{o}		53.56^{o}	10.36^{o}
	0.0625	32.22^{o}		53.62^{o}	10.23^{o}
	0.25	32.11^{o}		53.77^{o}	9.80^{o}
	1	32.00^{o}		54.48^{o}	8.54^{o}
	2	31.68^{o}		55.18^{o}	7.73^{o}
	4	30.80^{o}		56.01^{o}	7.65^{o}
	8	25.58^{o}		56.15^{o}	7.65^{o}
	16	4.36^{o}		56.15^{o}	7.61^{o}
79.15^{o}	0	90.00^{o}	78.87^{o}	57.25^{o}	
	0.00195	90.00^{o}	78.81^{o}	57.25^{o}	
	0.00781	90.00^{o}	78.64^{o}	57.18^{o}	
	0.0625	90.00^{o}	77.52^{o}	56.63^{o}	
	0.25	80.87^{o}	75.26^{o}	55.60^{o}	
	1	73.50^{o}	68.78^{o}	54.27^{o}	
	2	60.59^{o}	55.60^{o}	54.41^{o}	
	4	37.81^{o}	46.68^{o}	54.48^{o}	
	8	11.87^{o}	46.45^{o}	54.48^{o}	
	16	2.69^{o}	90.00^{o}	54.48^{o}	

Table II.

Comparison of exact and approximate scalar theory radiance values.

τ	μ_o	μ	ϕ	Downwelling or upwelling radiation	Scalar Theory	Stokes Vector Theory	Percent Difference
0.25	1	1	-	Up	2.8621 -3	2.8631 -3	0.03%
0.25	1	0.03785	-	Up	1.5092 -2	1.5089 -2	-0.02%
0.25	0.03785	0.89034	60°	Up	9.6381 -4	9.6367 -4	-0.01%
0.25	0.11333	0.99574	90°	Down	2.0010 -3	2.0006 -3	-0.02%
1	0.53786	0.89034	60°	Up	7.9171 -3	7.9146 -3	-0.03%
1	0.85332	0.11333	150°	Down	1.3534 -2	1.3528 -2	-0.04%
2	0.18816	1	30°	Up	3.7611 -3	3.7596 -3	-0.04%
2	0.11333	0.03785	90°	Down	6.3774 -4	6.3706 -4	-0.11%
4	0.53786	0.98574	60°	Up	9.7842 -3	9.7811 -3	-0.03%
4	0.85332	0.40452	180°	Down	9.6320 -3	9.6283 -3	-0.04%
8	0.18816	1	0°	Up	3.9351 -3	3.9336 -3	-0.04%
8	0.03785	0.11333	30°	Down	6.8123 -6	6.8172 -6	0.07%
16	0.53786	0.99574	120°	Up	9.2782 -3	9.2769 -3	-0.01%
16	0.18816	0.03785	150°	Down	5.9750 -7	5.9793 -7	0.07%

Table III.

Optical thickness	Solar zenith angle	Nadir angle of neutral points of reflected photons		Zenith angle of neutral points of transmitted photons	
		$\phi=180^o$	$\phi=180^o$	$\phi=0^o$	$\phi=0^o$
0.00195	31.43^o	31.4^o	31.4^o	57.0^o	5.6^o
0.00781		31.4^o	31.4^o	57.0^o	5.4^o
0.0625		31.6^o	31.3^o	57.0^o	5.3^o
0.25		31.8^o	31.2^o	57.1^o	5.7^o
1		32.5^o	30.5^o	57.5^o	6.5^o
2		33.6^o	29.3^o	57.8^o	7.2^o
4		34.0^o	28.8^o	57.9^o	9.6^o
8		34.0^o	28.8^o	43.4^o	28.1^o
16		34.0^o	28.8^o	-	-
		$\phi = 0^o$	$\phi=180^o$	$\phi=0^o$	$\phi=0^o$
0.00195	79.15^o	75.2^o	78.8^o; 79.6^o	53.6^o	-
0.00781		75.2^o	75.5^o; 80.7^o	53.6^o	-
0.0625		75.0^o	76.7^o; 82.0^o	53.8^o	-
0.25		75.2^o	75.6^o; 83.4^o	54.2^o	-
1		75.8^o	75.1^o; 83.9^o	54.6^o	-
2		75.9^o	75.2^o; 83.7^o	57.6^o	70.1^o
4		75.9^o	75.2^o; 83.7^o	-	-
8		75.9^o	75.2^o; 83.7^o	-	-
16		75.9^o	75.2^o; 83.7^o	-	-

Captions for Figures

Fig. 1. Upward radiance reflected from a plane parallel layer with Rayleigh phase matrix as a function of the cosine of the nadir angle μ. The cosine of the solar zenith angle $\mu_o = 1$; the surface albedo $A = 0$. Curves are given for layers with various values of the optical thickness τ. The incoming solar flux is normalized to unity in a direction perpendicular to the solar beam.

Fig. 2. Downward radiance transmitted through a plane parallel layer with Rayleigh scattering as a function of the cosine of the zenith angle μ. $\mu_o = 1$; $A = 0$.

Fig. 3. $\Delta R/R$ (where R is exact radiance from Stokes vector; ΔR is the exact radiance minus the approximate scalar radiance) for the reflected light from a Rayleigh scattering layer for $\mu_o = 1$, $A = 0$.

Fig. 4. $\Delta R/R$ (see caption to Fig. 3) for the transmitted light through a Rayleigh scattering layer for $\mu_o = 1$, $A = 0$.

Fig. 5. Single scattering function obtained from phase matrix for haze L (continental haze) as a function of the scattering angle.

Fig. 6. Upward radiance reflected from a plane parallel haze L layer as a function of the cosine of the nadir angle μ for $\mu_o = 0.85332$, $A = 0$. The left hand portion of the graph is for an azimuthal angle $\phi = 0^o$ and the right hand portion for $\phi = 180^o$. The solar horizon is at the left of the figure, the nadir at the center followed by the antisolar point and the antisolar horizon at the right. Curves are given for layers with various values of the optical thickness τ.

Fig. 7. Downward radiance transmitted through a haze L layer as a function of the cosine of the zenith angle μ for $\mu_o = 0.85332$, $A = 0$. The azimuthal angle $\phi = 0^o$ for the left hand portion of the graph and

180° for the right. The solar horizon is at the left of the figure, followed by the solar point, the zenith, and the antisolar horizon on the right.

Fig. 8. Upward radiance for haze L, $\mu_o = 0.18817$, A = 0, and $\phi = 0^{\circ}$ and 180°. (See caption to Fig. 6).

Fig. 9. Downward radiance for haze L, $\mu_o = 0.18817$, A = 0, and $\phi = 0^{\circ}$ and 180°. (See caption to Fig. 7).

Fig. 10. Polarization of the upward radiation for Rayleigh scattering for $\mu_o = 0.18817$, A = 0, and $\phi = 0^{\circ}$ and 180° for layers of various optical thicknesses. (See caption to Fig. 6).

Fig. 11. Position of Babinet, Brewster, and Arago neutral points for upward radiation reflected from a Rayleigh scattering layer when $\mu_o = 0.85332$, 0.111333, and 0.03785 and A = 0 and 1. The ordinate is the cosine of the nadir angle and the abscissa is the optical thickness of the reflecting layer. The Brewster point appears between the antisolar direction and the antisolar horizon and the Arago point appears between the solar horizon and the nadir.

Fig. 12. Position of Babinet, Brewster, and Arago neutral points for upward radiation reflected from a Rayleigh scattering layer when $\mu_o = 0.53786$ and 0.18817 and A = 0, 0.2, and 1. (See caption to Fig. 11).

Fig. 13. Polarization of the downward radiation transmitted through Rayleigh scattering layers of various optical thicknesses for $\mu_o = 0.18817$, A = 0, and $\phi = 0^{\circ}$ and 180°. (See caption to Fig. 7).

Fig. 14. Position of Babinet and Brewster neutral points for downward radiation transmitted through a Rayleigh scattering layer when $\mu_o = 0.85332$ and A = 0, 0.2, and 1. The ordinate is the cosine of the zenith angle and the abscissa is the optical thickness of the transmitting layer.

Fig. 15. Position of Babinet, Brewster, and Arago neutral points for downward radiation transmitted through a Rayleigh scattering layer when $\mu_o = 0.53786$ and A = 0, 0.2, and 1. The Brewster point appears between the solar direction and the solar horizon while the Arago point appears between the antisolar horizon and the zenith. The ordinate is the cosine of the zenith angle and the abscissa is the optical thickness of the transmitting layer.

Fig. 16. Position of Babinet, Brewster, and Arago neutral points for downward radiation transmitted through a Rayleigh scattering layer when $\mu_o = 0.18817$ and A = 0 and 1. (See caption to Fig. 15).

Fig. 17. Position of Babinet, Brewster, and Arago neutral points for downward radiation transmitted through a Rayleigh scattering layer when $\mu_o = 0.03785$ and A = 0 and 1. (See caption to Fig. 15).

Fig. 18. Polarization of single scattered photons from haze L. The two insets show the polarization for scattering angles near 0^o. The abscissa is the cosine of the scattering angle.

Fig. 19. Angles at which the polarization of single scattered photons from haze L is zero. Each curve is for a particular value of the cosine of the solar zenith angle μ_o. The ordinate is the cosine of the zenith angle μ and the abscissa is the azimuthal angle ϕ. The upper part of the figure is for photons reflected into an upward direction, while the lower part is for photons transmitted through the scattering layer in a downward direction.

Fig. 20. Polarization of the upward radiation for haze L, $\mu_o = 0.85332$, A = 0, and $\phi = 0^o$ and 180^o (upper curves) and $\phi = 30^o$ and 150^o (lower curves) for layers of various optical thicknesses. (See caption to Fig. 6).

Fig. 21. Position of Rayleigh-like neutral points for photons reflected from a haze L layer. Curves are given for five different solar zenith

angles. The ordinate is the cosine of the nadir angle and the abiscissa is the optical thickness of the reflecting layer.

Fig. 22. Polarization of the upward and downward radiation for haze L for $\mu_o = 0.85332$, A = 0, and $\phi = 90^o$ for layers of various optical thicknesses. (See captions to Figs. 6 and 7).

Fig. 23. Polarization of the upward radiation for haze L, $\mu_o = 0.188166$, A = 0, and $\phi = 0^o$ and 180^o for layers of various optical thicknesses. (See caption to Fig. 6).

Fig. 24. Polarization of the downward radiation for haze L, $\mu_o = 0.85332$, A = 0, and $\phi = 0^o$ and 180^o for layers of various optical thicknesses. (See caption to Fig. 7).

Fig. 25. Polarization of the downward radiation for haze L for $\mu_o = 0.85332$, A = 0, and $\phi = 30^o$ and 150^o for layers of various optical thicknesses. (See caption to Fig. 7).

Fig. 26. Polarization of the downward radiation for haze L for $\mu_o = 0.188166$, A = 0, and $\phi = 0^o$ and 180^o for layers of various optical thicknesses. (See caption to Fig. 7).

Fig. 27. Position of non-Rayleigh-like neutral points for photons transmitted through a haze L layer. Curves are given for six different solar zenith angles. The ordinate is the cosine of the zenith angle and the abscissa is the optical thickness of the scattering layer.

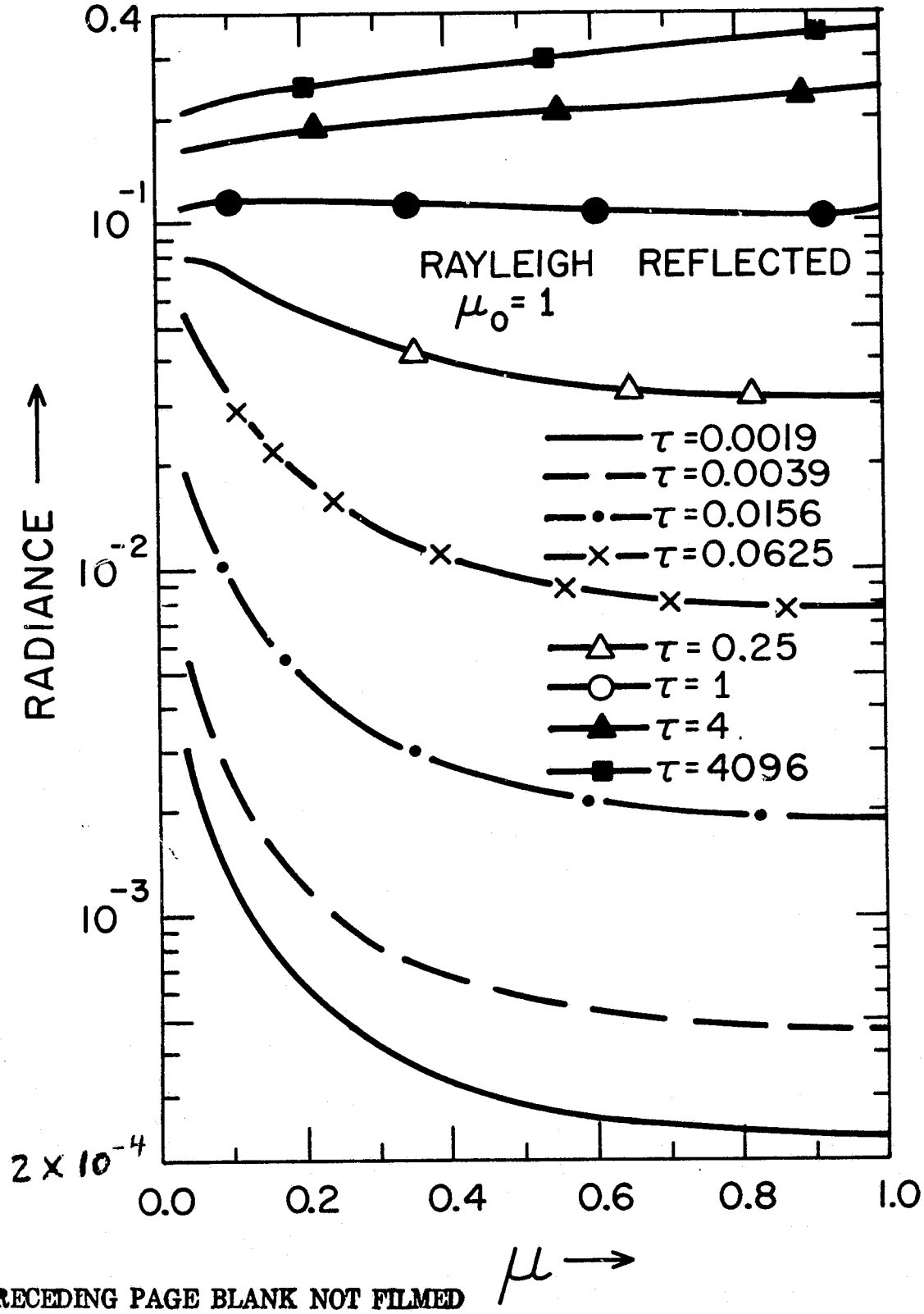

PRECEDING PAGE BLANK NOT FILMED

Fig. 1

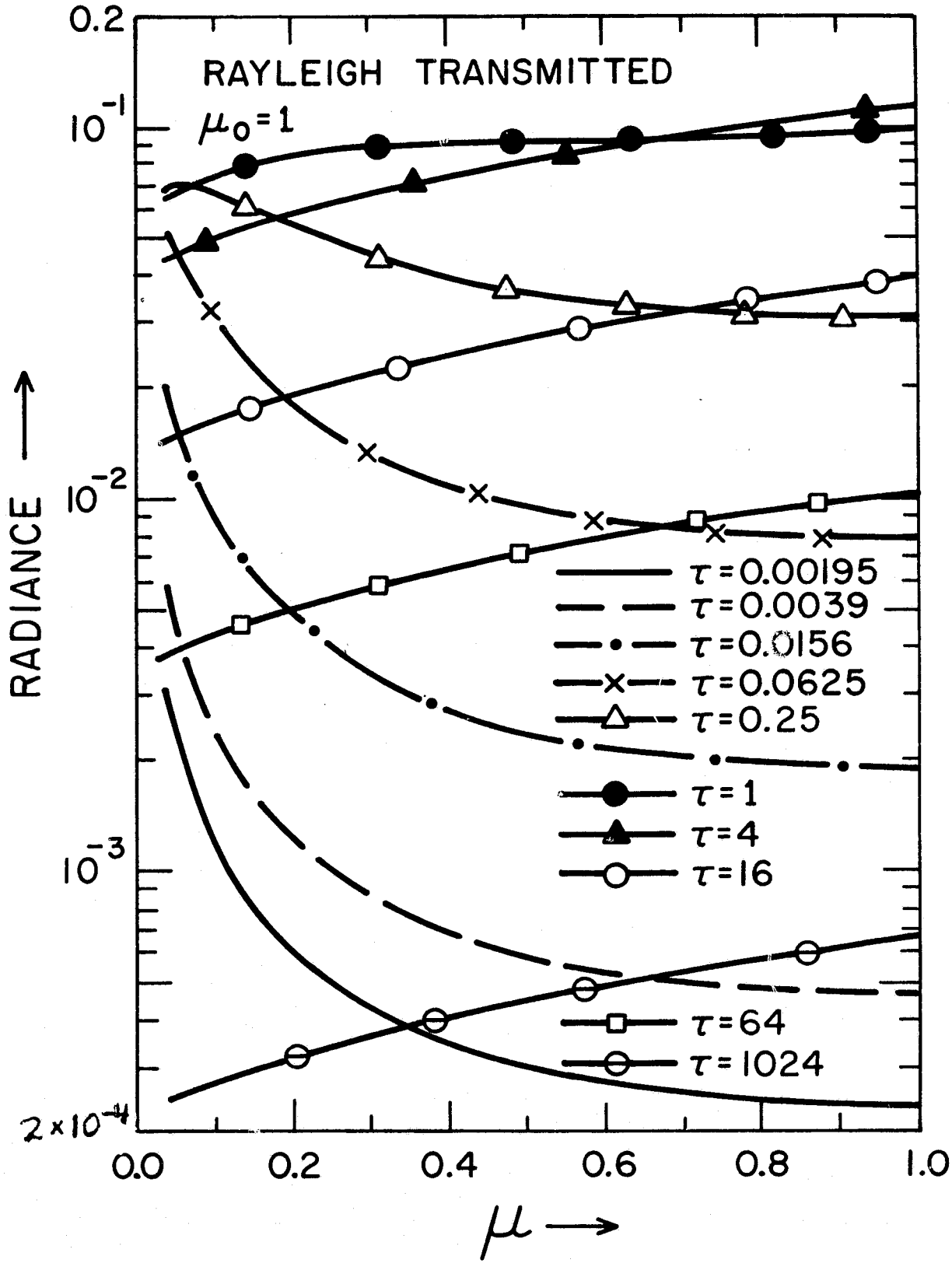
RAYLEIGH TRANSMITTED
$\mu_0 = 1$
0.2
10^{-1}
10^{-2}
10^{-3}
2×10^{-4}
RADIANCE
0.0
0.2
0.4
0.6
0.8
1.0
μ
$\tau = 0.00195$
$\tau = 0.0039$
$\tau = 0.0156$
$\tau = 0.0625$
$\tau = 0.25$
$\tau = 1$
$\tau = 4$
$\tau = 16$
$\tau = 64$
$\tau = 1024$

Fig. 2

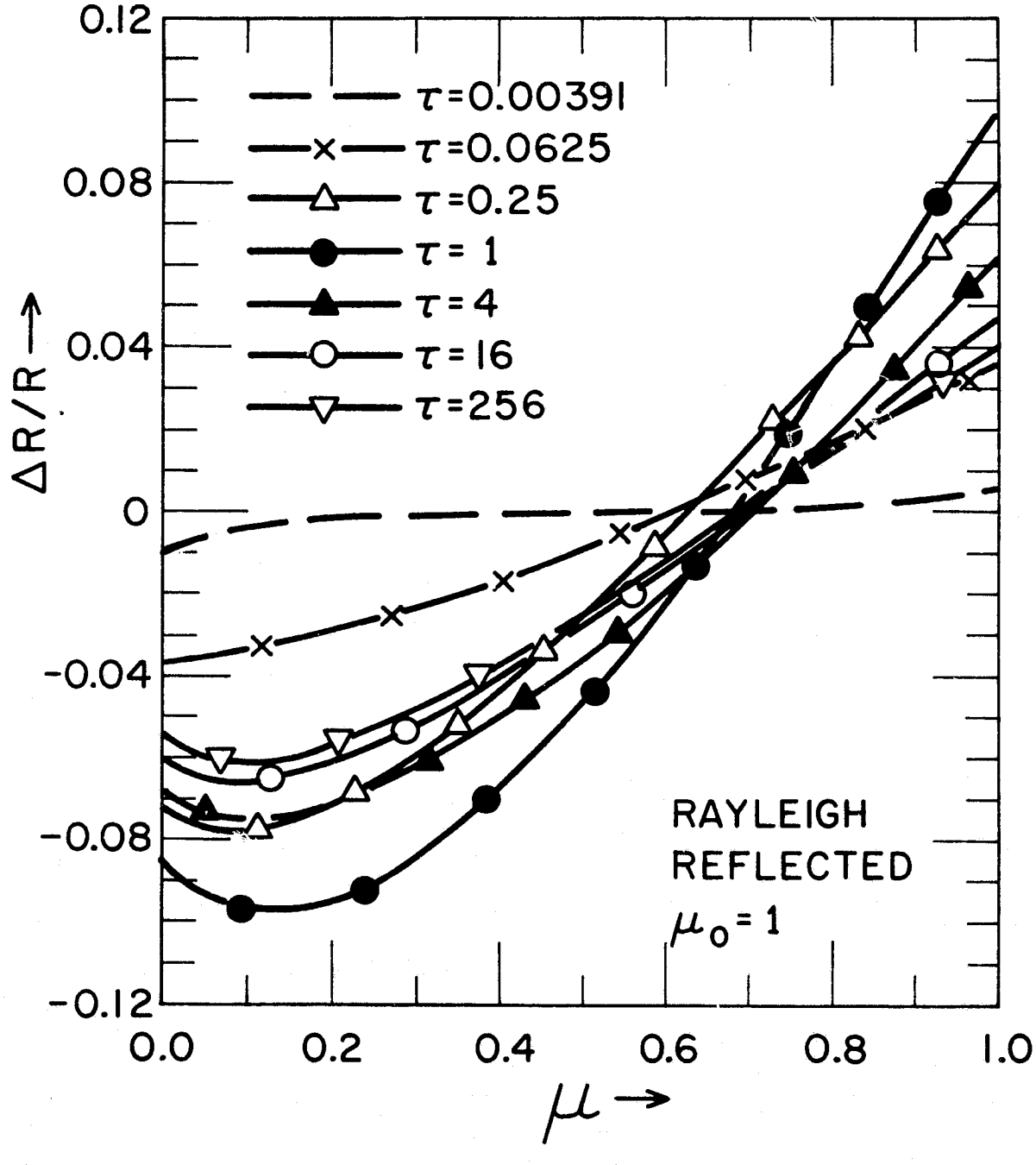
0.12
0.08
0.04
0
-0.04
-0.08
-0.12
ΔR/R →
τ=0.00391
τ=0.0625
τ=0.25
τ= 1
τ=4
τ=16
τ=256
RAYLEIGH
REFLECTED
μ0 = 1
0.0
0.2
0.4
0.6
0.8
1.0
μ →

Fig. 3

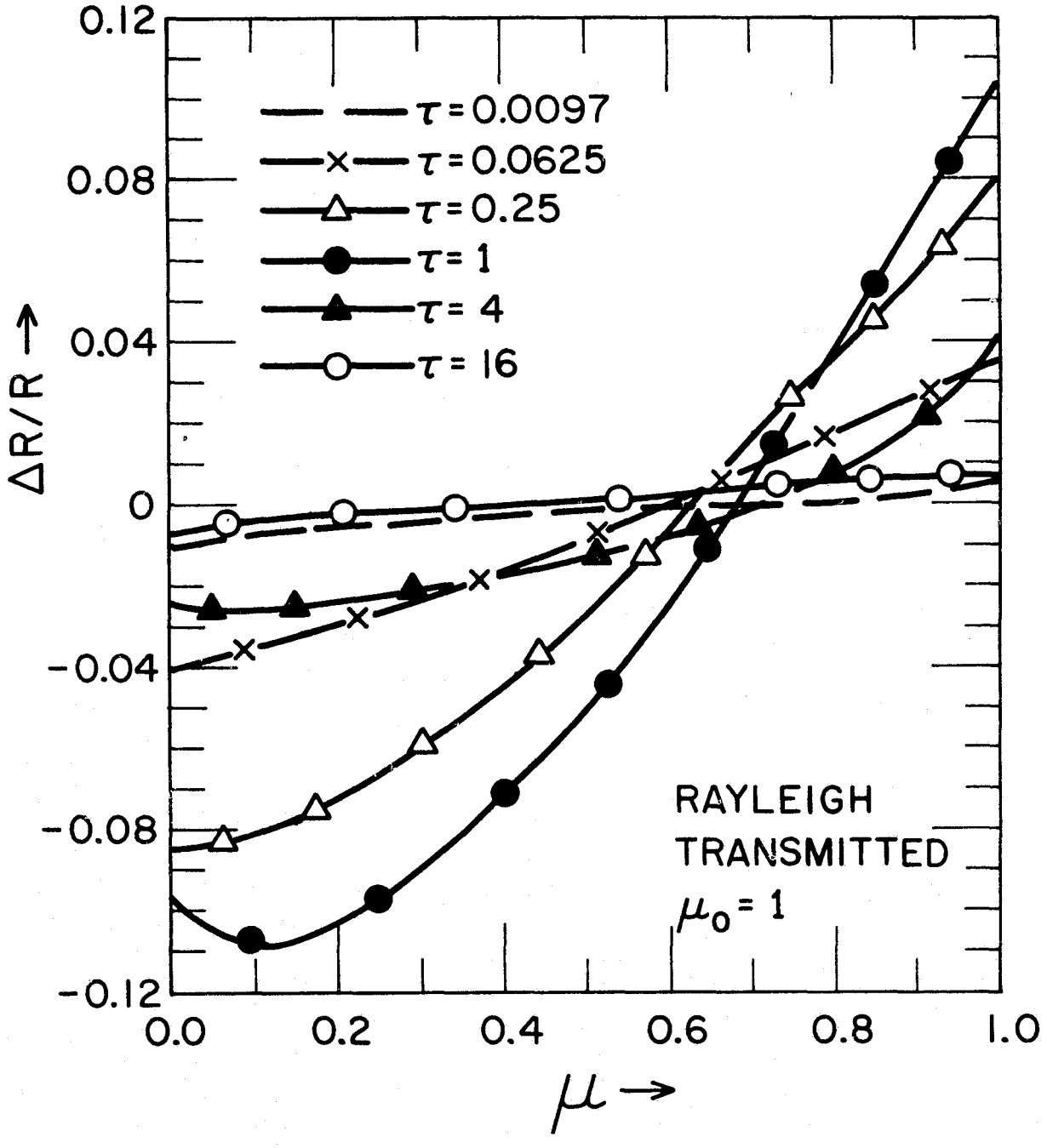
0.12
0.08
0.04
0
-0.04
-0.08
-0.12
ΔR/R →
τ = 0.0097
τ = 0.0625
τ = 0.25
τ = 1
τ = 4
τ = 16
RAYLEIGH
TRANSMITTED
μ0 = 1
0.0
0.2
0.4
0.6
0.8
1.0
μ →

Fig. 4

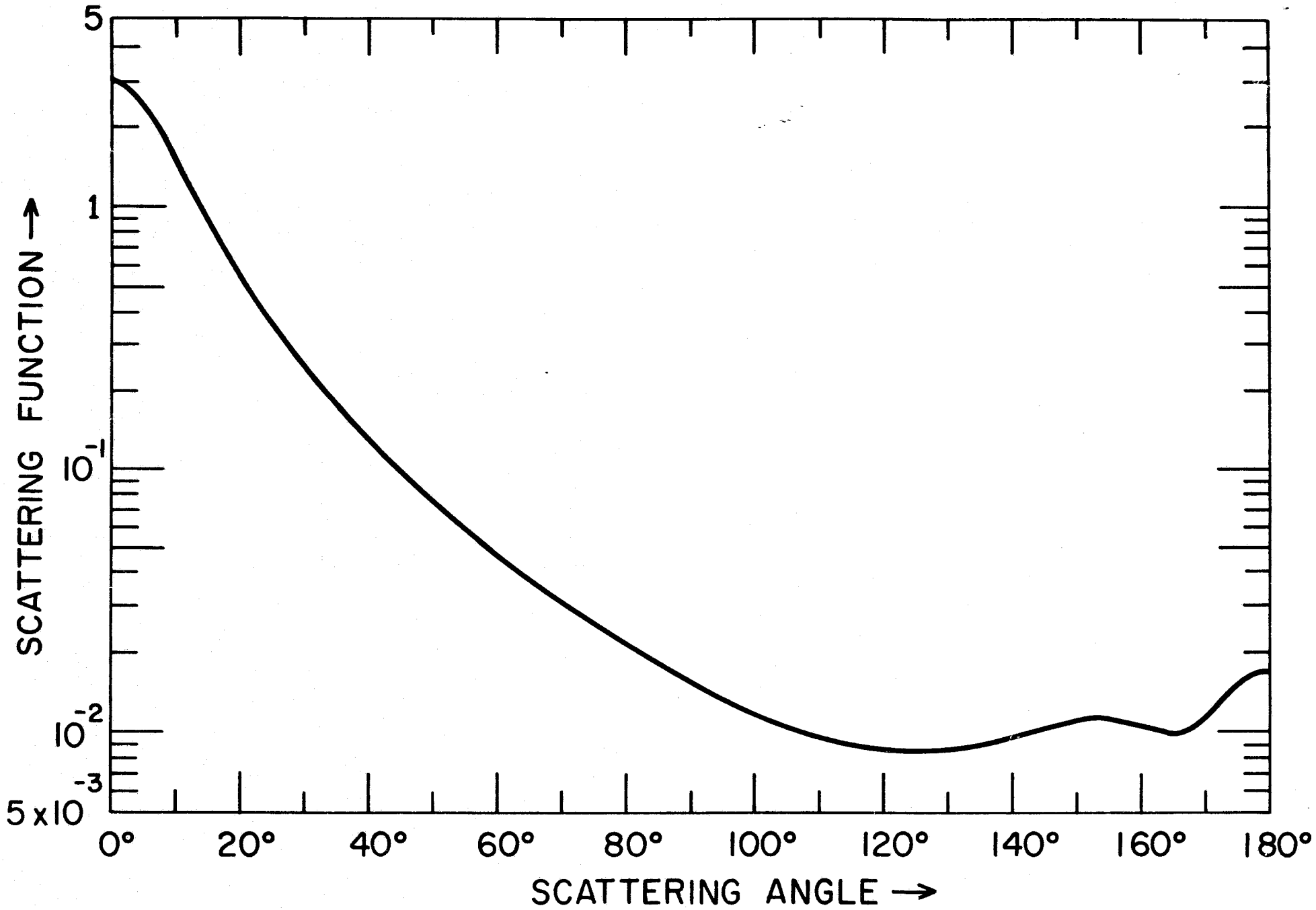
5
1
10^{-1}
10^{-2}
5×10^{-3}
SCATTERING FUNCTION →
0°
20°
40°
60°
80°
100°
120°
140°
160°
180°
SCATTERING ANGLE →

Fig. 5

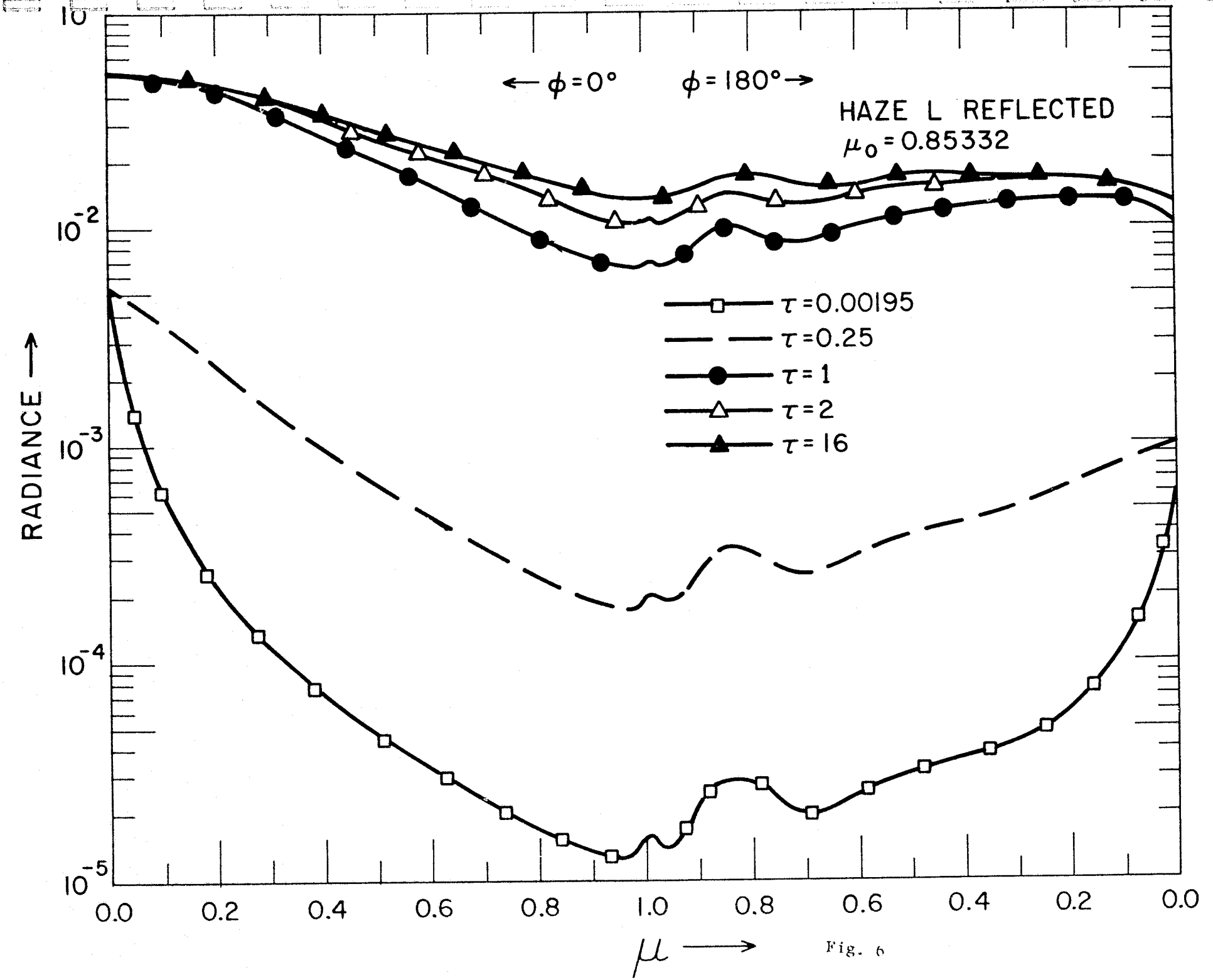
← φ=0°
φ=180°→
HAZE L REFLECTED
μ0 = 0.85332
τ=0.00195
τ=0.25
τ=1
τ=2
τ=16
RADIANCE →
10
10-2
10-3
10-4
10-5
0.0
0.2
0.4
0.6
0.8
1.0
0.8
0.6
0.4
0.2
0.0
μ →

Fig. 6

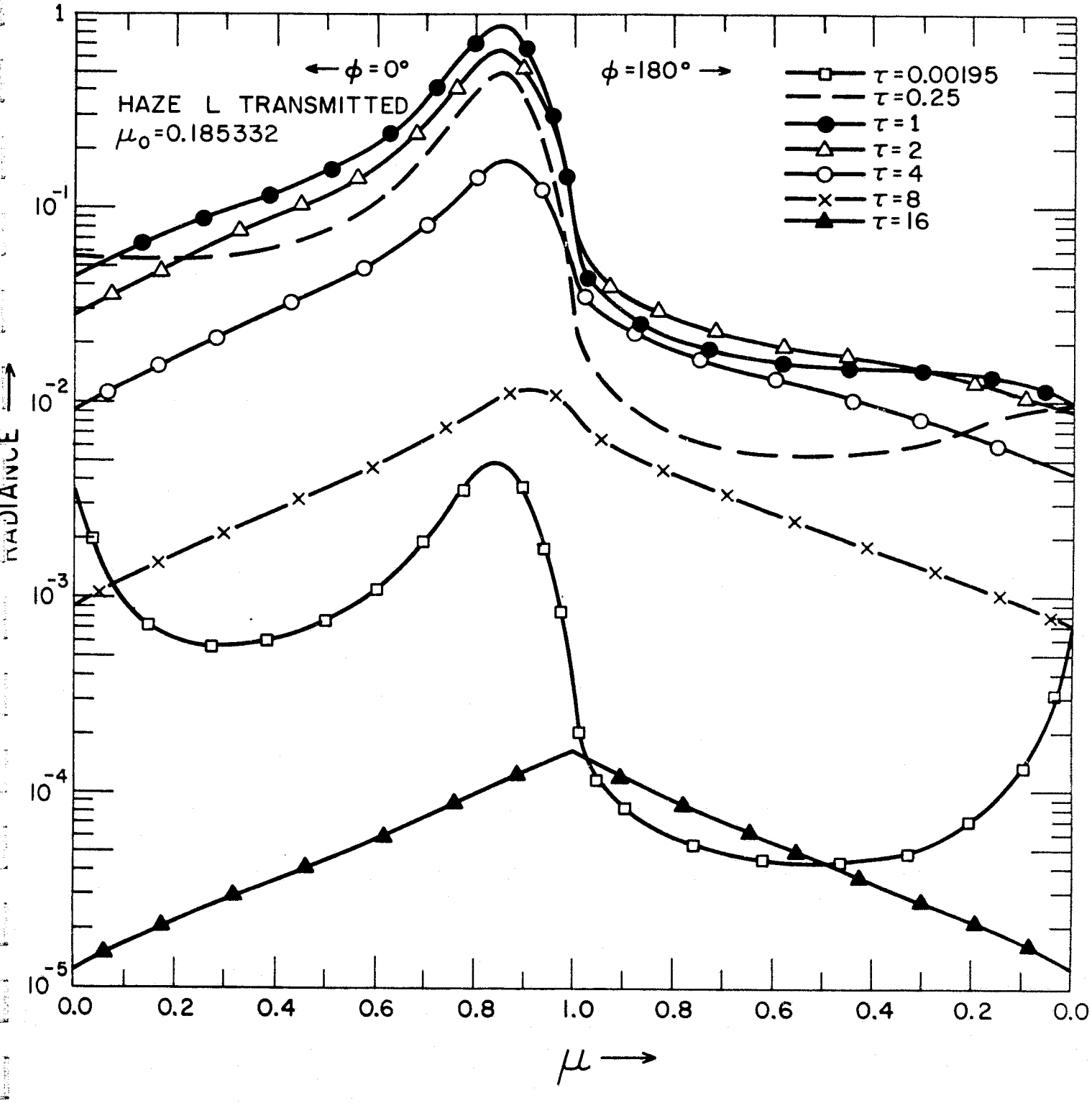
HAZE L TRANSMITTED
μ_0=0.185332
← ϕ = 0°
ϕ = 180° →
τ = 0.00195
τ = 0.25
τ = 1
τ = 2
τ = 4
τ = 8
τ = 16
RADIANCE →
1
10^{-1}
10^{-2}
10^{-3}
10^{-4}
10^{-5}
0.0
0.2
0.4
0.6
0.8
1.0
0.8
0.6
0.4
0.2
0.0
μ →

Fig. 7

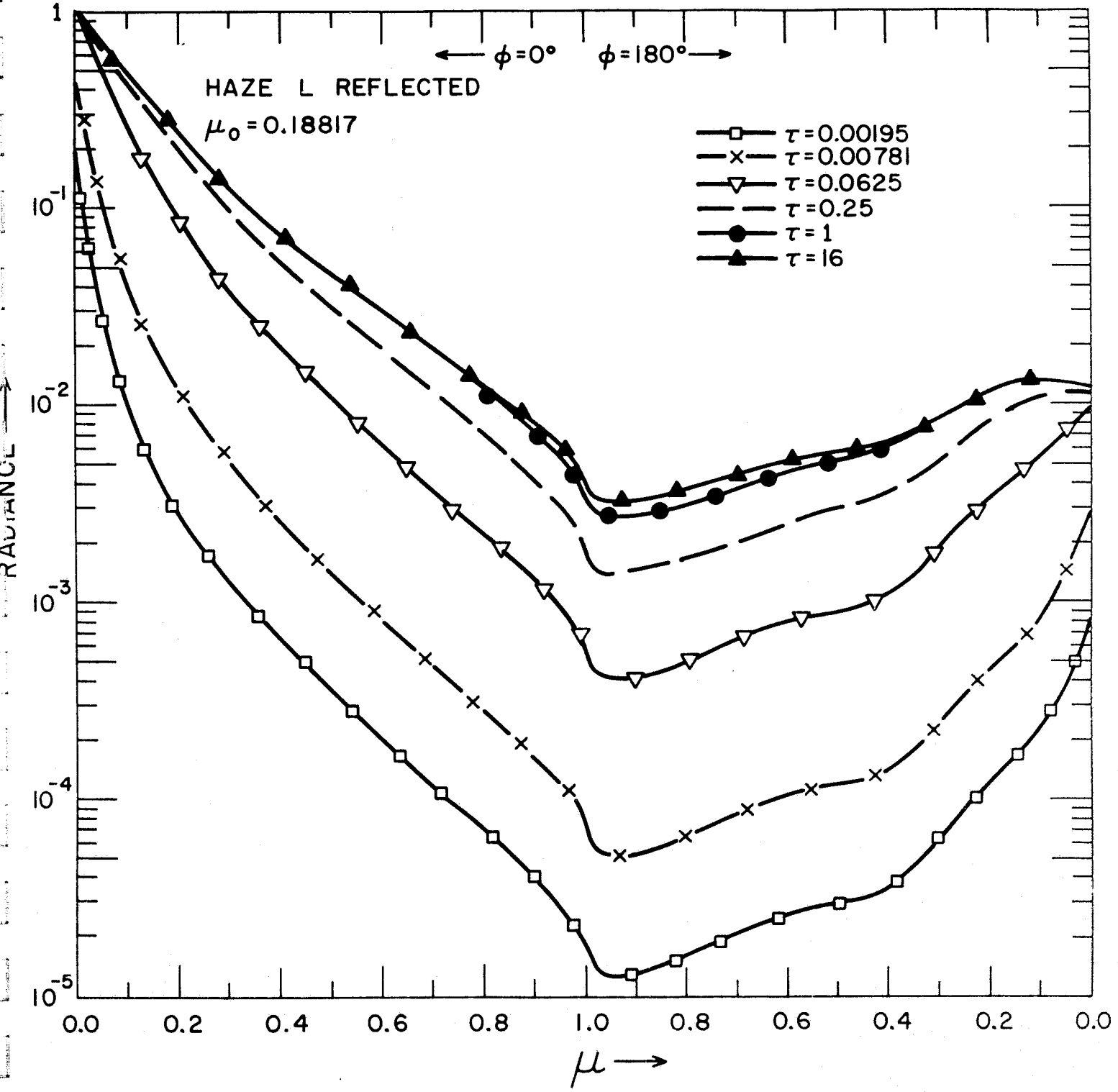
← φ=0° φ=180°→
HAZE L REFLECTED
μ₀ = 0.18817
τ = 0.00195
τ = 0.00781
τ = 0.0625
τ = 0.25
τ = 1
τ = 16
RADIANCE →
1
10⁻¹
10⁻²
10⁻³
10⁻⁴
10⁻⁵
0.0
0.2
0.4
0.6
0.8
1.0
0.8
0.6
0.4
0.2
0.0
μ →

Fig. 8

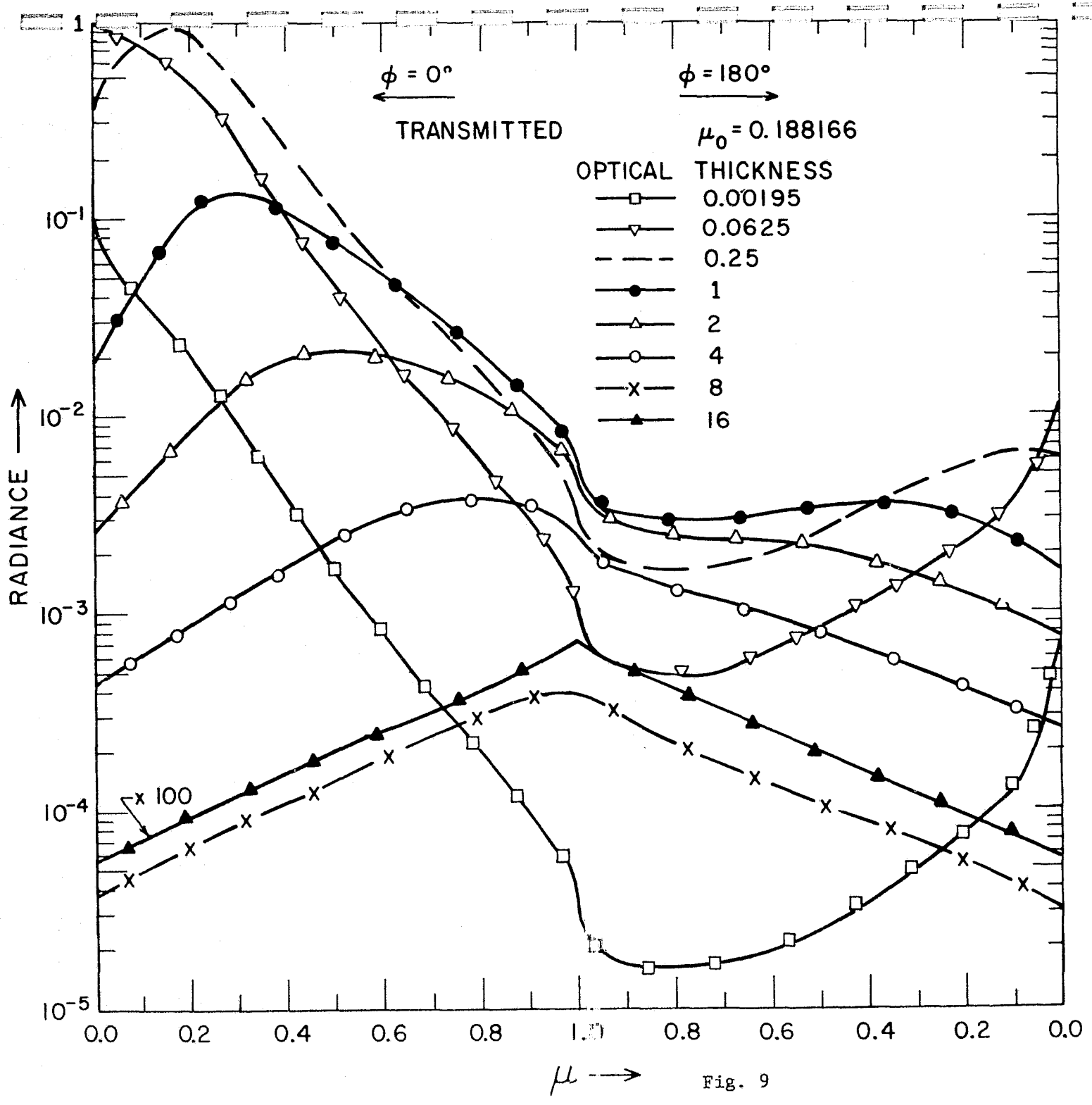
$\phi = 0°$
$\phi = 180°$
TRANSMITTED
$\mu_0 = 0.188166$
OPTICAL THICKNESS
0.00195
0.0625
0.25
1
2
4
8
16
x 100
RADIANCE
1
10^{-1}
10^{-2}
10^{-3}
10^{-4}
10^{-5}
0.0
0.2
0.4
0.6
0.8
1.0
0.8
0.6
0.4
0.2
0.0
μ

Fig. 9

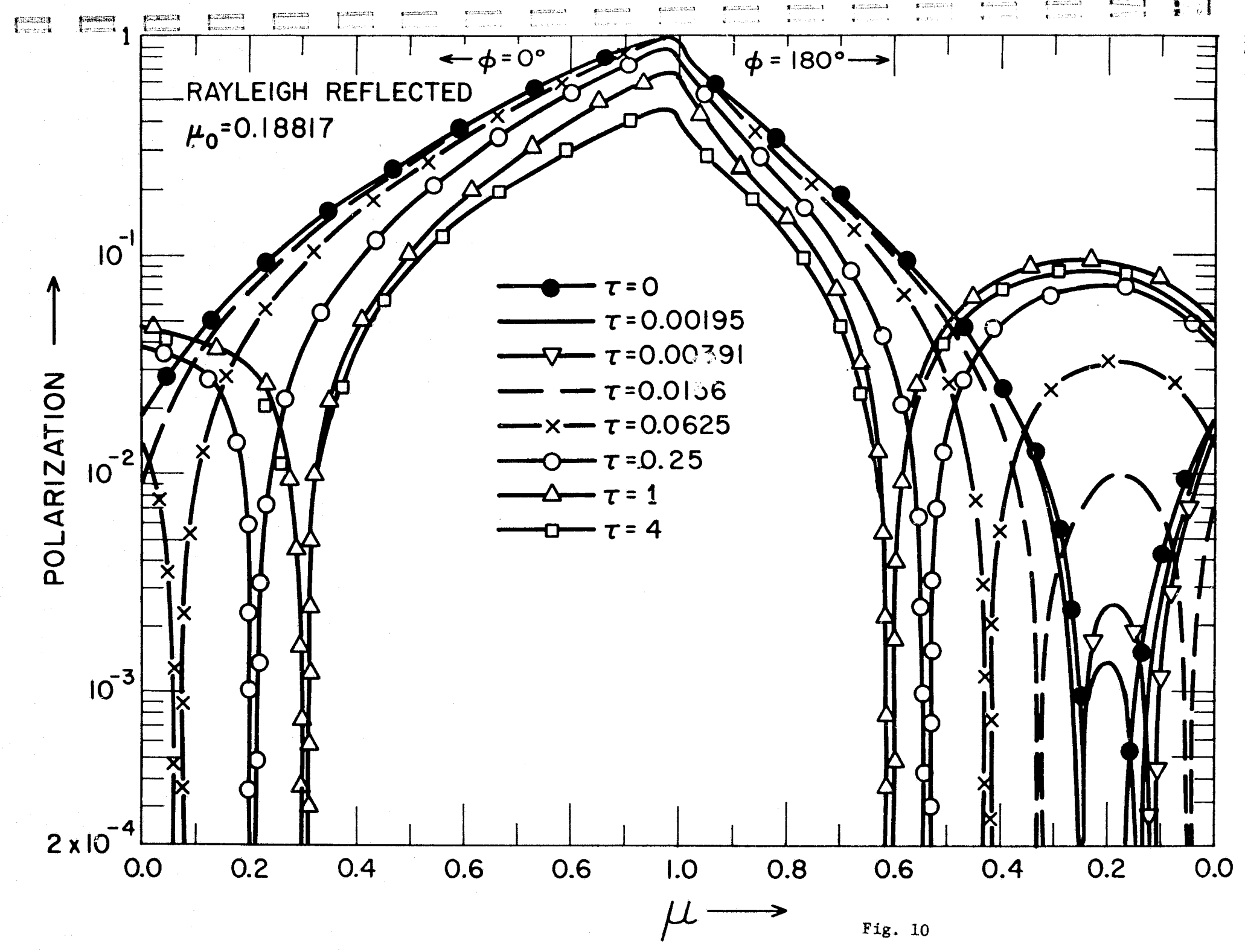
RAYLEIGH REFLECTED
μ_0=0.18817
← ϕ = 0°
ϕ = 180° →
τ = 0
τ = 0.00195
τ = 0.00391
τ = 0.0156
τ = 0.0625
τ = 0.25
τ = 1
τ = 4
POLARIZATION →
1
10^{-1}
10^{-2}
10^{-3}
2×10^{-4}
0.0
0.2
0.4
0.6
0.6
1.0
0.8
0.6
0.4
0.2
0.0
μ →

Fig. 10

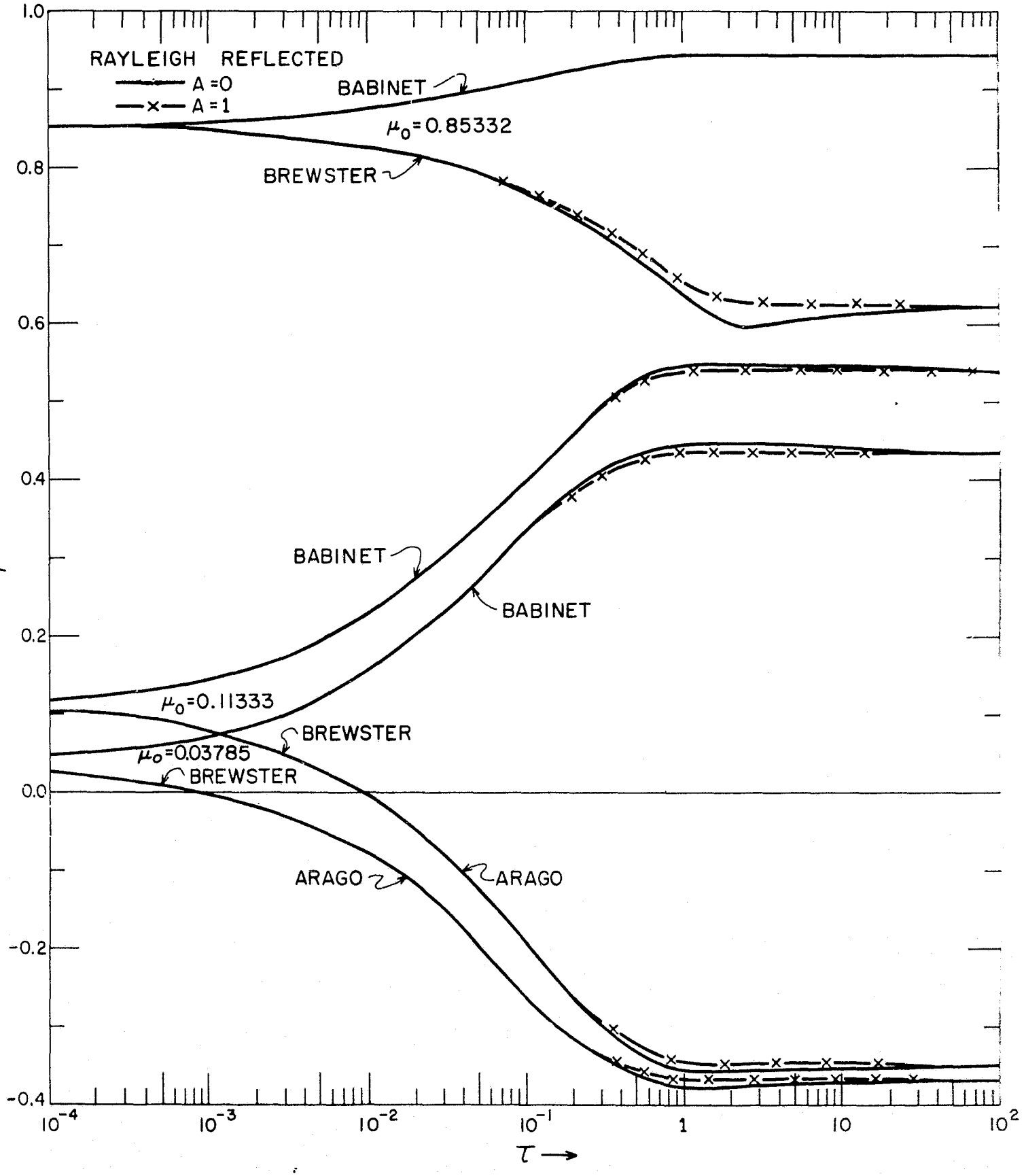
RAYLEIGH REFLECTED
A=0
A=1
BABINET
μ_0=0.85332
BREWSTER
BABINET
BABINET
μ_0=0.11333
BREWSTER
μ_0=0.03785
BREWSTER
ARAGO
ARAGO
1.0
0.8
0.6
0.4
0.2
0.0
-0.2
-0.4
10^{-4}
10^{-3}
10^{-2}
10^{-1}
1
10
10^2
τ →

Fig. 11

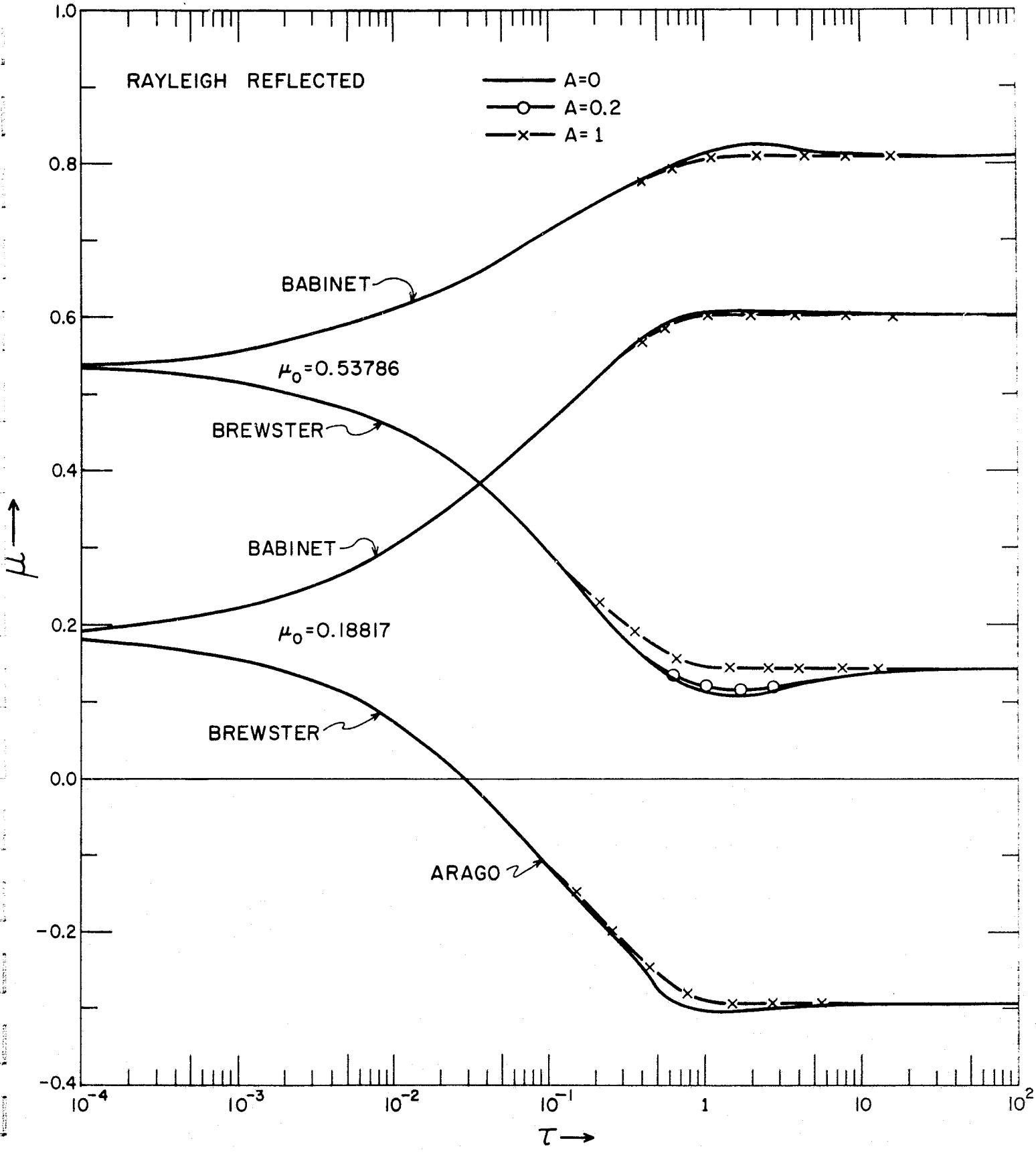
RAYLEIGH REFLECTED
A=0
A=0.2
A= 1
BABINET
μ_0=0.53786
BREWSTER
BABINET
μ_0=0.18817
BREWSTER
ARAGO
1.0
0.8
0.6
0.4
0.2
0.0
-0.2
-0.4
μ
10^{-4}
10^{-3}
10^{-2}
10^{-1}
1
10
10^{2}
τ

Fig. 12

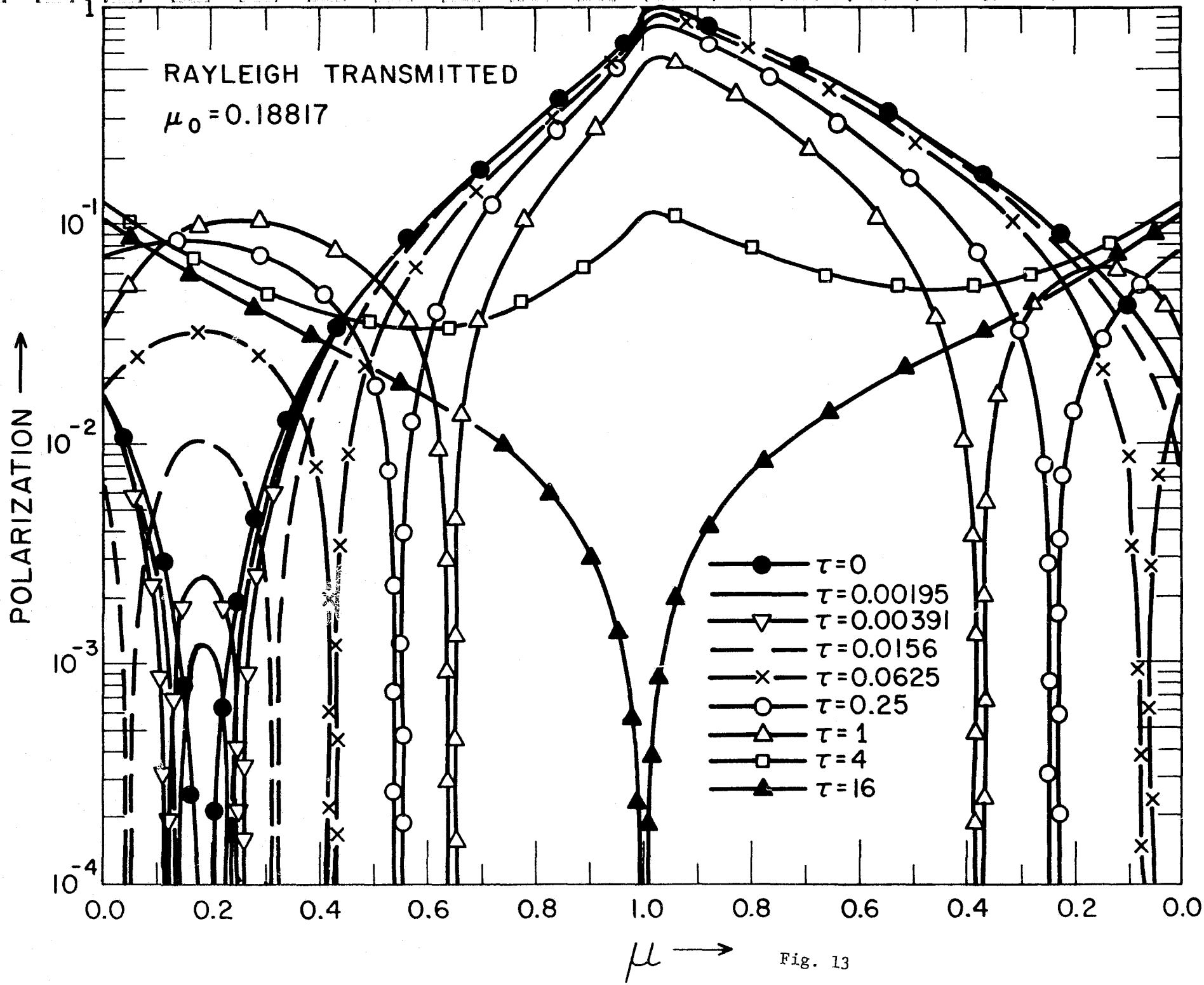
RAYLEIGH TRANSMITTED
$\mu_0 = 0.18817$
POLARIZATION
μ
1
10^{-1}
10^{-2}
10^{-3}
10^{-4}
0.0
0.2
0.4
0.6
0.8
1.0
$\tau = 0$
$\tau = 0.00195$
$\tau = 0.00391$
$\tau = 0.0156$
$\tau = 0.0625$
$\tau = 0.25$
$\tau = 1$
$\tau = 4$
$\tau = 16$

Fig. 13

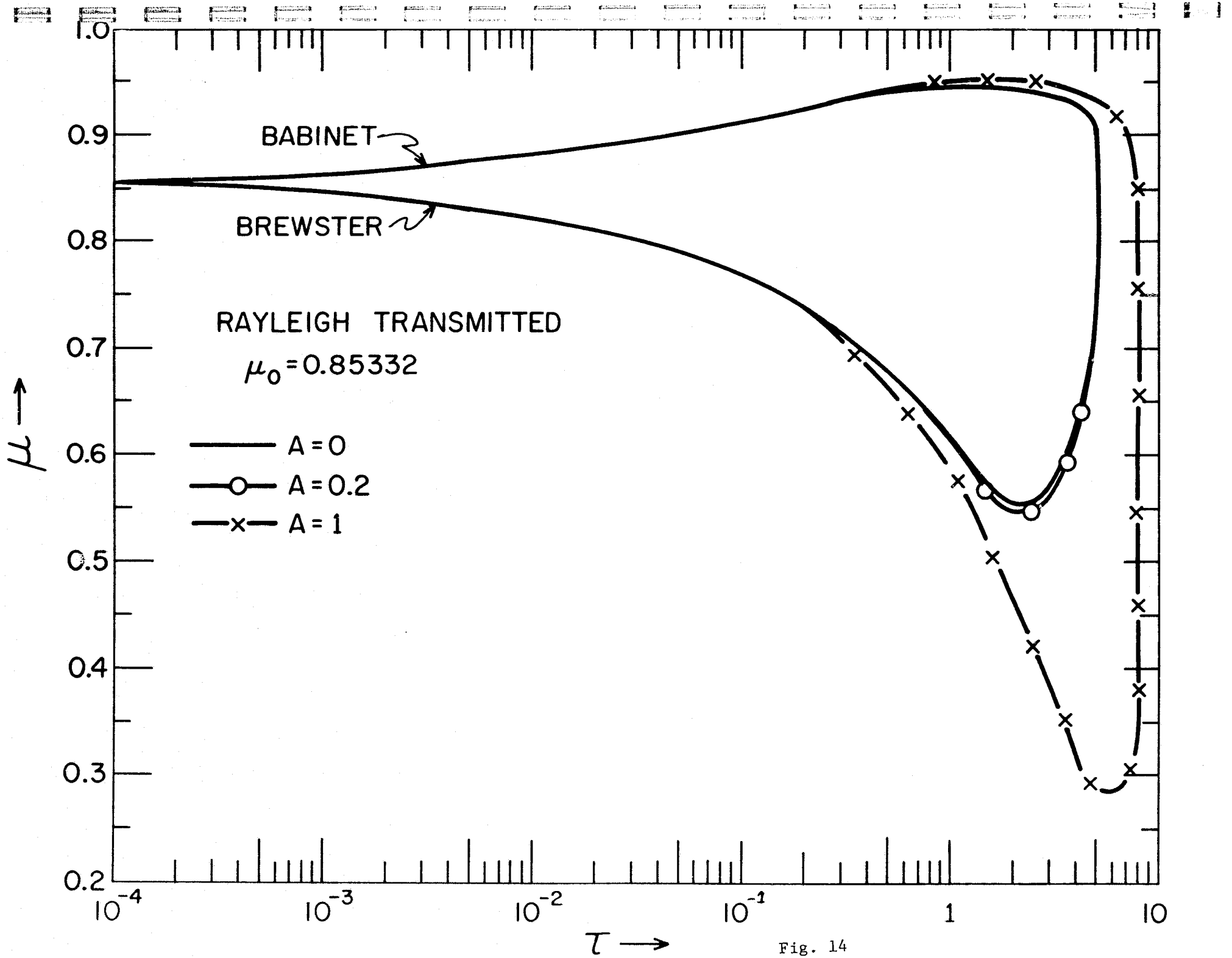
1.0
0.9
0.8
0.7
0.6
0.5
0.4
0.3
0.2
BABINET
BREWSTER
RAYLEIGH TRANSMITTED
$\mu_0 = 0.85332$
A = 0
A = 0.2
A = 1
$\mu \rightarrow$
10^{-4}
10^{-3}
10^{-2}
10^{-1}
1
10
$\tau \rightarrow$

Fig. 14

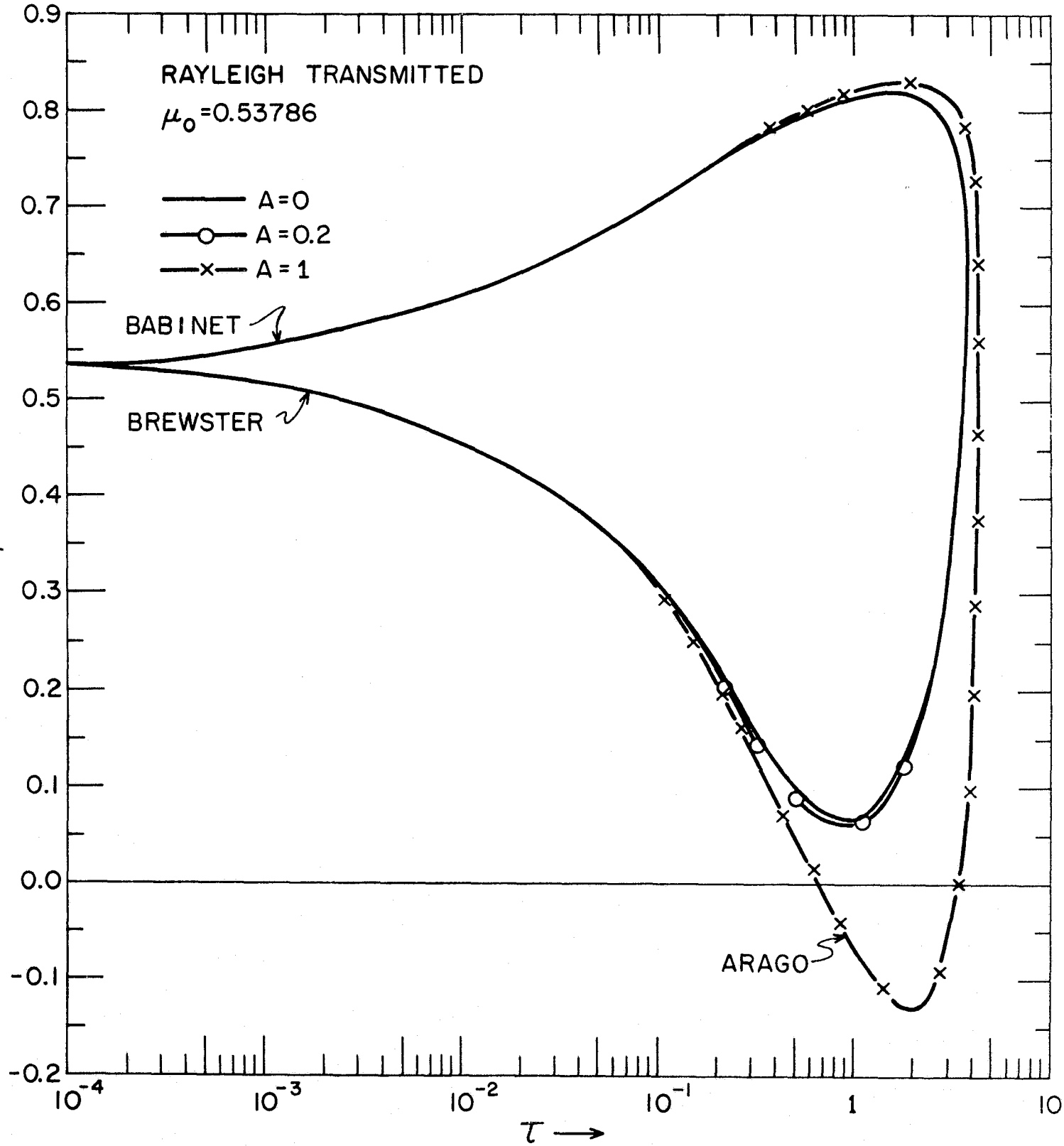
RAYLEIGH TRANSMITTED
μ_0=0.53786
A=0
A=0.2
A=1
BABINET
BREWSTER
ARAGO
0.9
0.8
0.7
0.6
0.5
0.4
0.3
0.2
0.1
0.0
-0.1
-0.2
μ
10^{-4}
10^{-3}
10^{-2}
10^{-1}
1
10
τ

Fig. 15

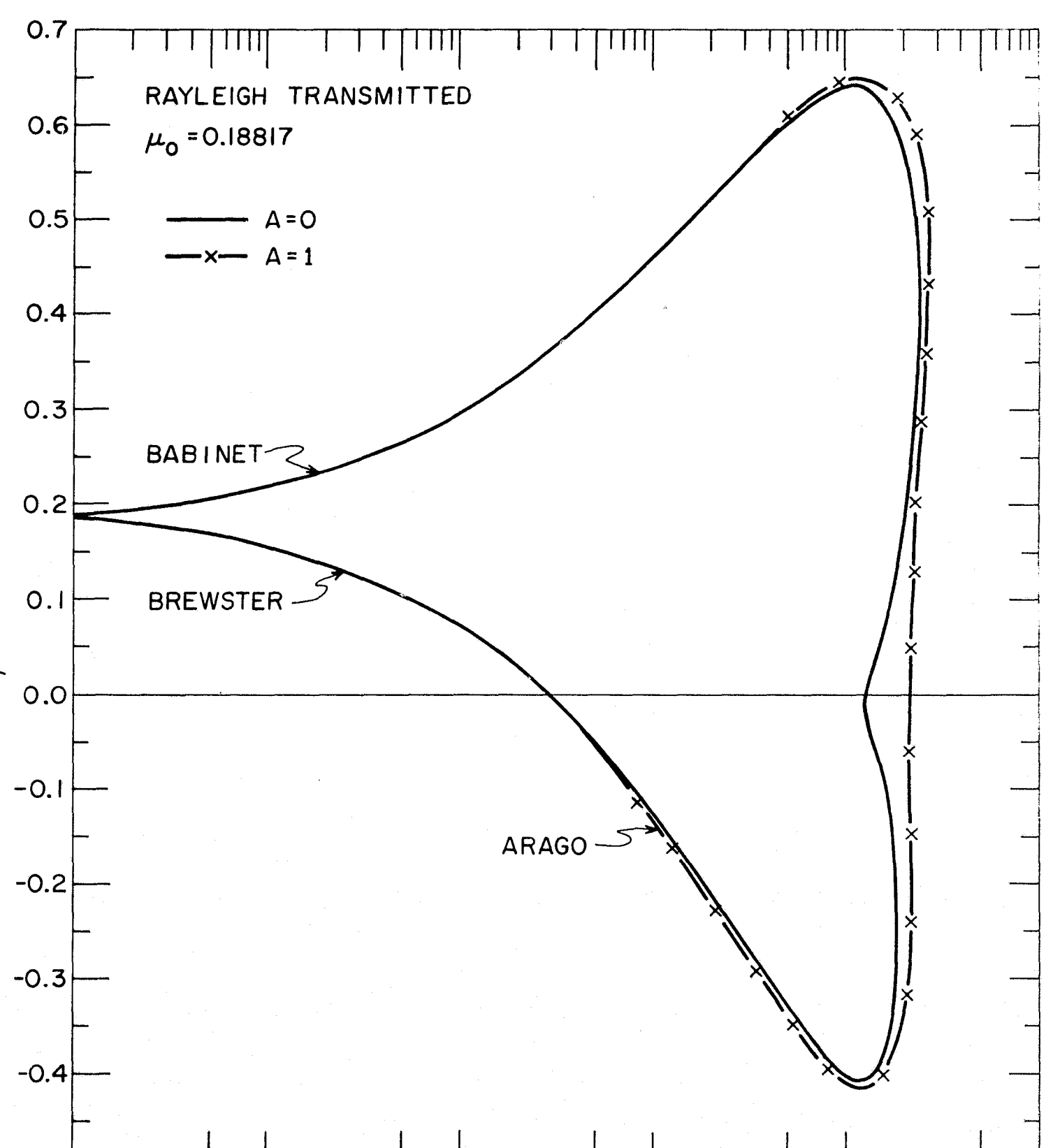
RAYLEIGH TRANSMITTED
$\mu_0 = 0.18817$
A=0
A=1
BABINET
BREWSTER
ARAGO
0.7
0.6
0.5
0.4
0.3
0.2
0.1
0.0
-0.1
-0.2
-0.3
-0.4
-0.5
10^{-4}
10^{-3}
10^{-2}
10^{-1}
1
10
$\mu \rightarrow$
$\tau \rightarrow$

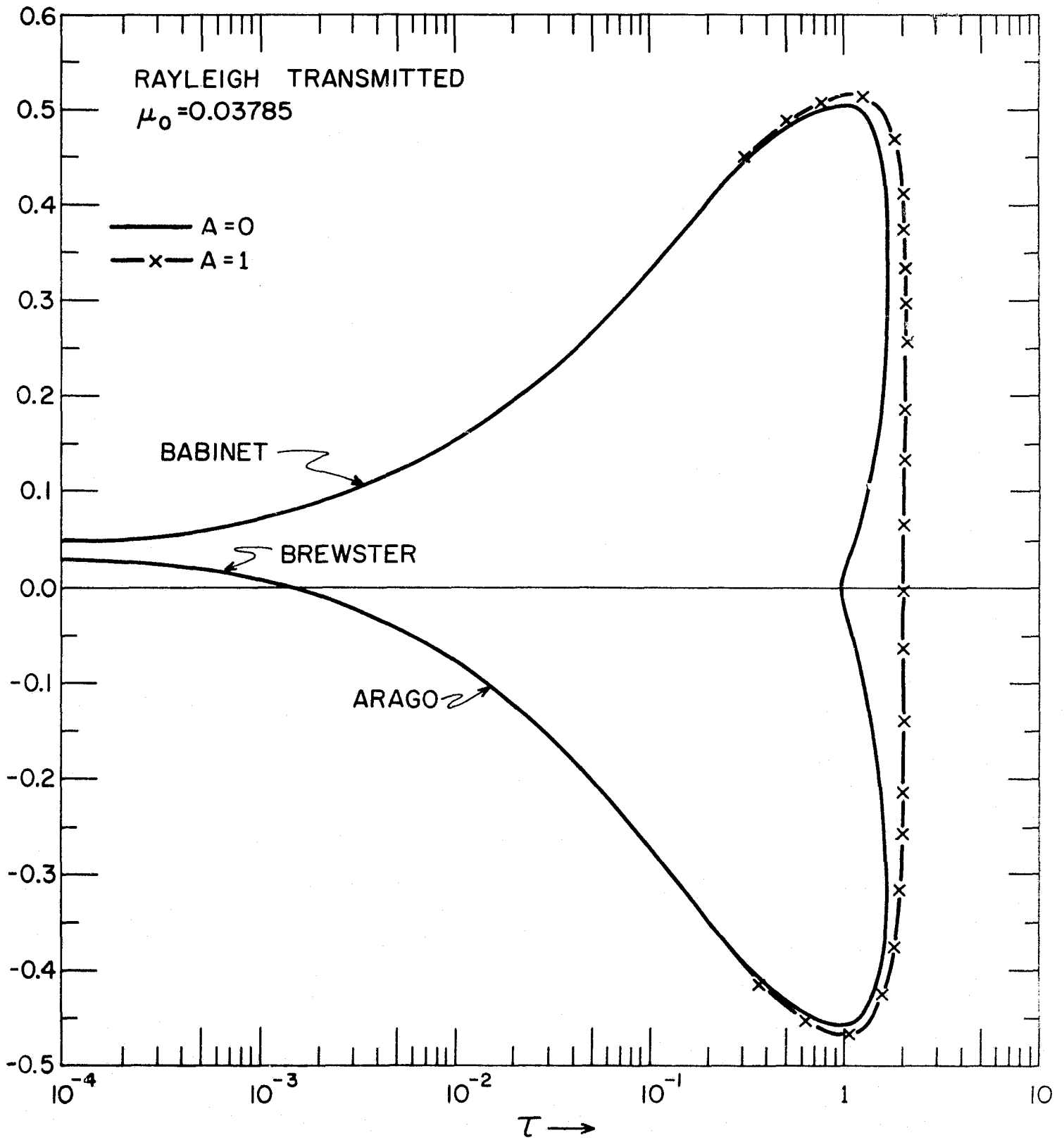
RAYLEIGH TRANSMITTED
μ_0=0.03785
A=0
A=1
BABINET
BREWSTER
ARAGO
0.6
0.5
0.4
0.3
0.2
0.1
0.0
-0.1
-0.2
-0.3
-0.4
-0.5
10^{-4}
10^{-3}
10^{-2}
10^{-1}
1
10
τ →

Fig. 17

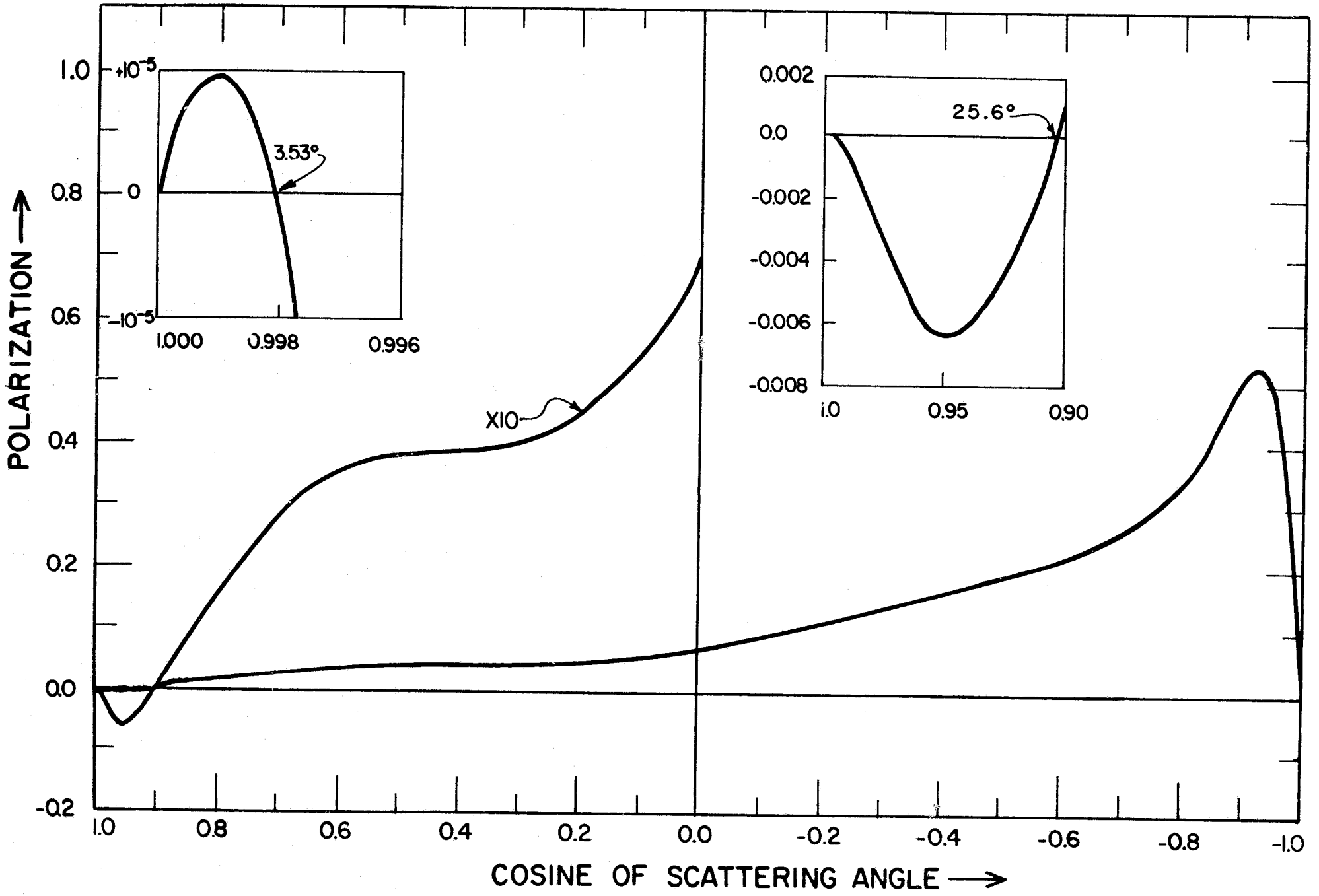
POLARIZATION ⟶
COSINE OF SCATTERING ANGLE ⟶
1.0
0.8
0.6
0.4
0.2
0.0
-0.2
-0.4
-0.6
-0.8
-1.0
X10
+10⁻⁵
0
-10⁻⁵
3.53°
1.000
0.998
0.996
0.002
0.0
-0.002
-0.004
-0.006
-0.008
25.6°
1.0
0.95
0.90

Fig. 18

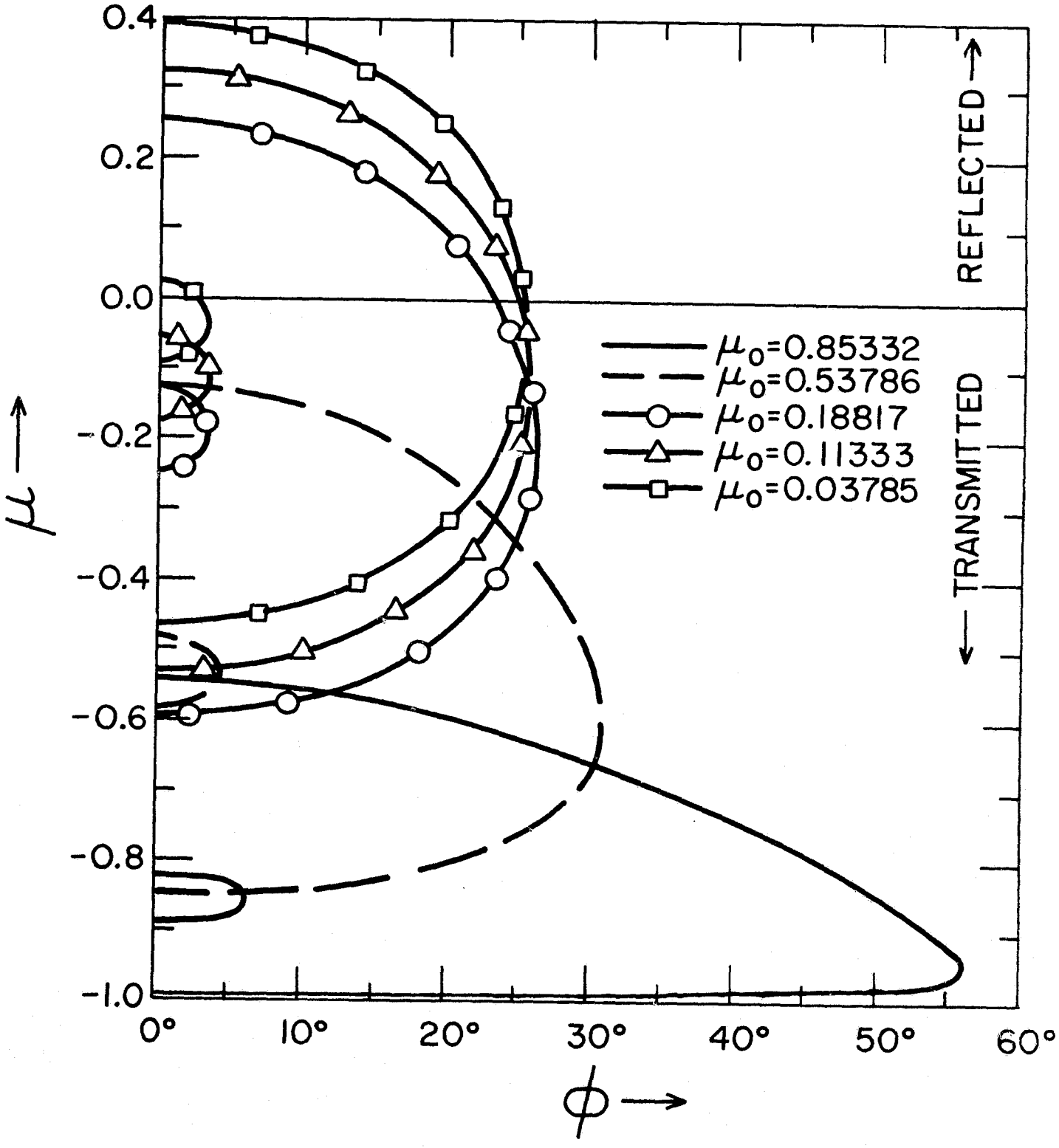
0.4
0.2
0.0
-0.2
-0.4
-0.6
-0.8
-1.0
μ
0°
10°
20°
30°
40°
50°
60°
φ
REFLECTED
TRANSMITTED
μ0=0.85332
μ0=0.53786
μ0=0.18817
μ0=0.11333
μ0=0.03785

Fig. 19

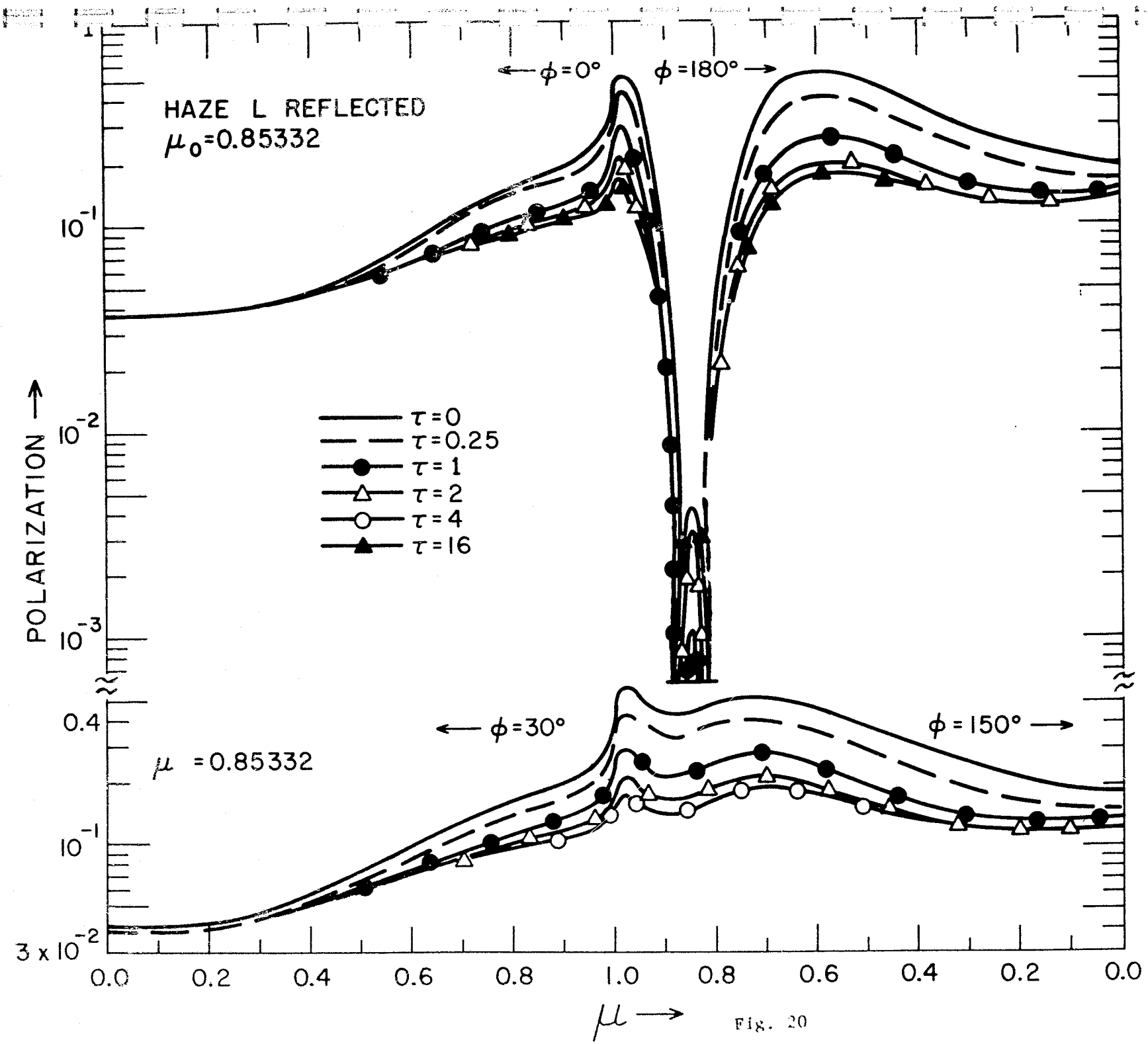
HAZE L REFLECTED
μ_0=0.85332
ϕ=0°
ϕ=180°
τ=0
τ=0.25
τ=1
τ=2
τ=4
τ=16
POLARIZATION
10^{-1}
10^{-2}
10^{-3}
0.4
10^{-1}
3×10^{-2}
ϕ=30°
ϕ=150°
μ =0.85332
0.0
0.2
0.4
0.6
0.8
1.0
0.8
0.6
0.4
0.2
0.0
μ

Fig. 20

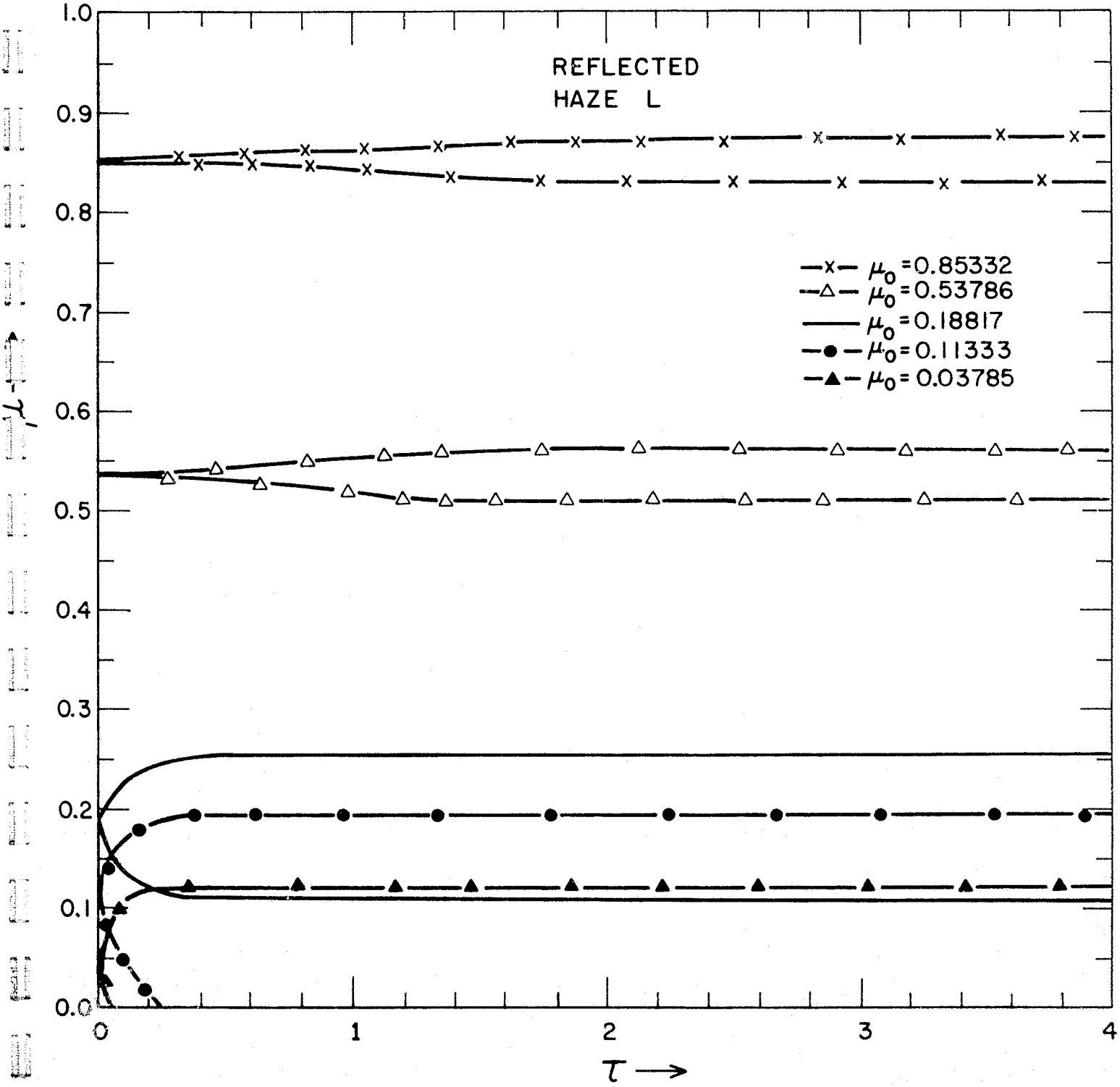
REFLECTED
HAZE L
—x— μ_0 = 0.85332
—△— μ_0 = 0.53786
—— μ_0 = 0.18817
—●— μ_0 = 0.11333
—▲— μ_0 = 0.03785
1.0
0.9
0.8
0.7
0.6
0.5
0.4
0.3
0.2
0.1
0.0
0
1
2
3
4
τ →
μ →

Fig. 21

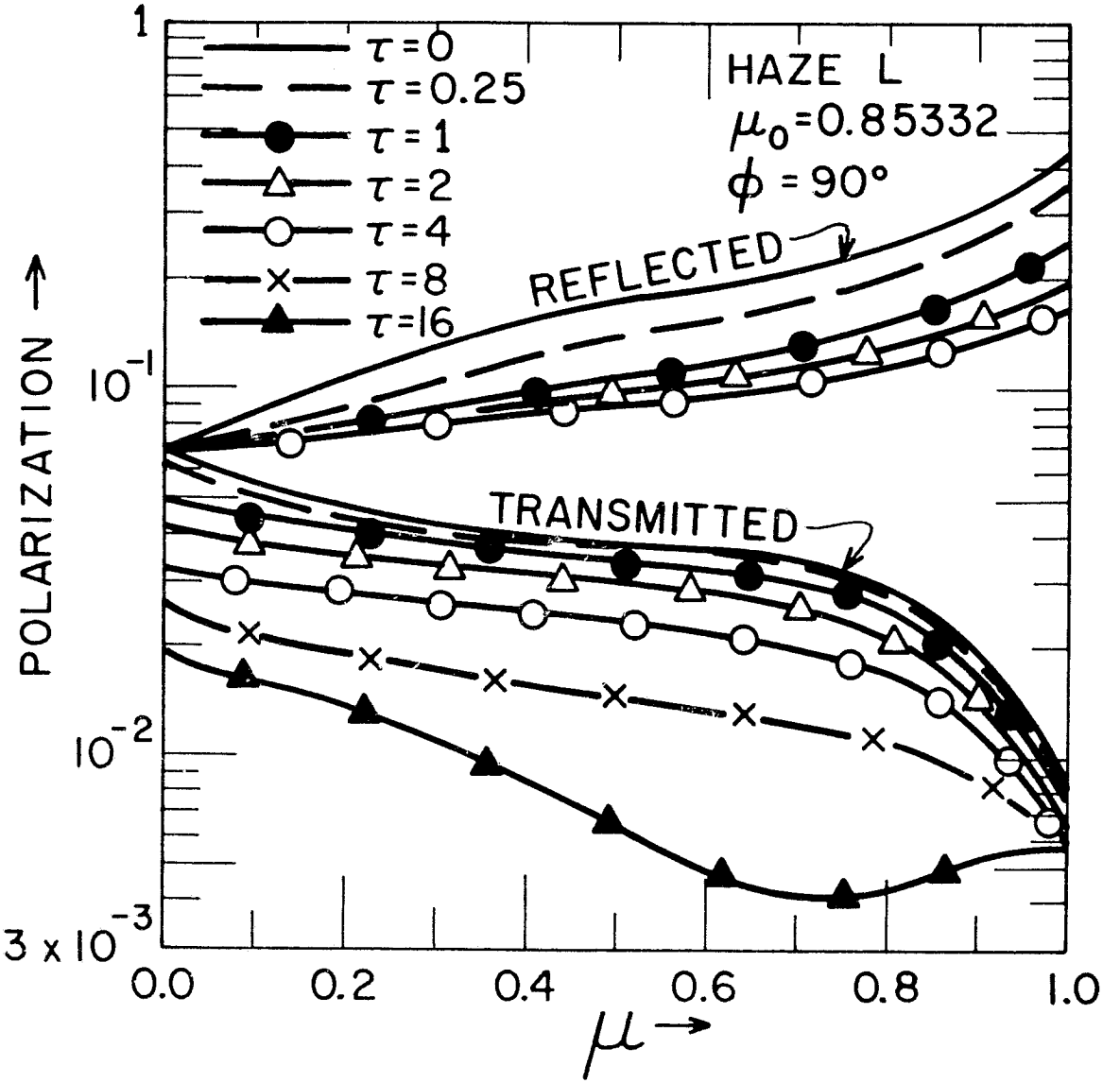
τ=0
τ=0.25
τ=1
τ=2
τ=4
τ=8
τ=16
HAZE L
μ0=0.85332
φ = 90°
REFLECTED
TRANSMITTED
POLARIZATION →
1
10-1
10-2
3 x 10-3
0.0
0.2
0.4
0.6
0.8
1.0
μ →

Fig. 22

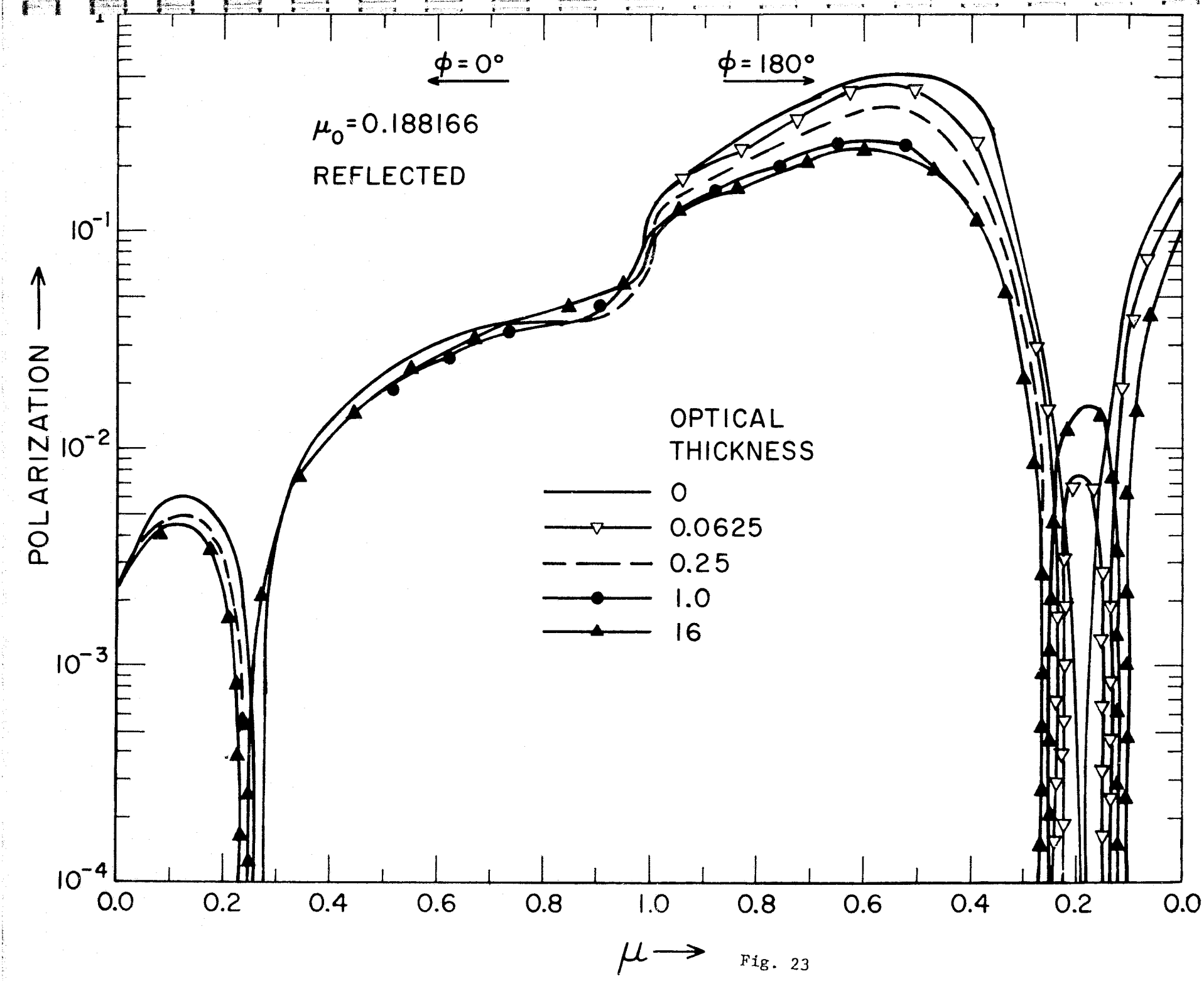
$\phi = 0°$
$\phi = 180°$
$\mu_0 = 0.188166$
REFLECTED
OPTICAL THICKNESS
0
0.0625
0.25
1.0
16
POLARIZATION ⟶
10^{-1}
10^{-2}
10^{-3}
10^{-4}
0.0
0.2
0.4
0.6
0.8
1.0
0.8
0.6
0.4
0.2
0.0
$\mu \longrightarrow$

Fig. 23

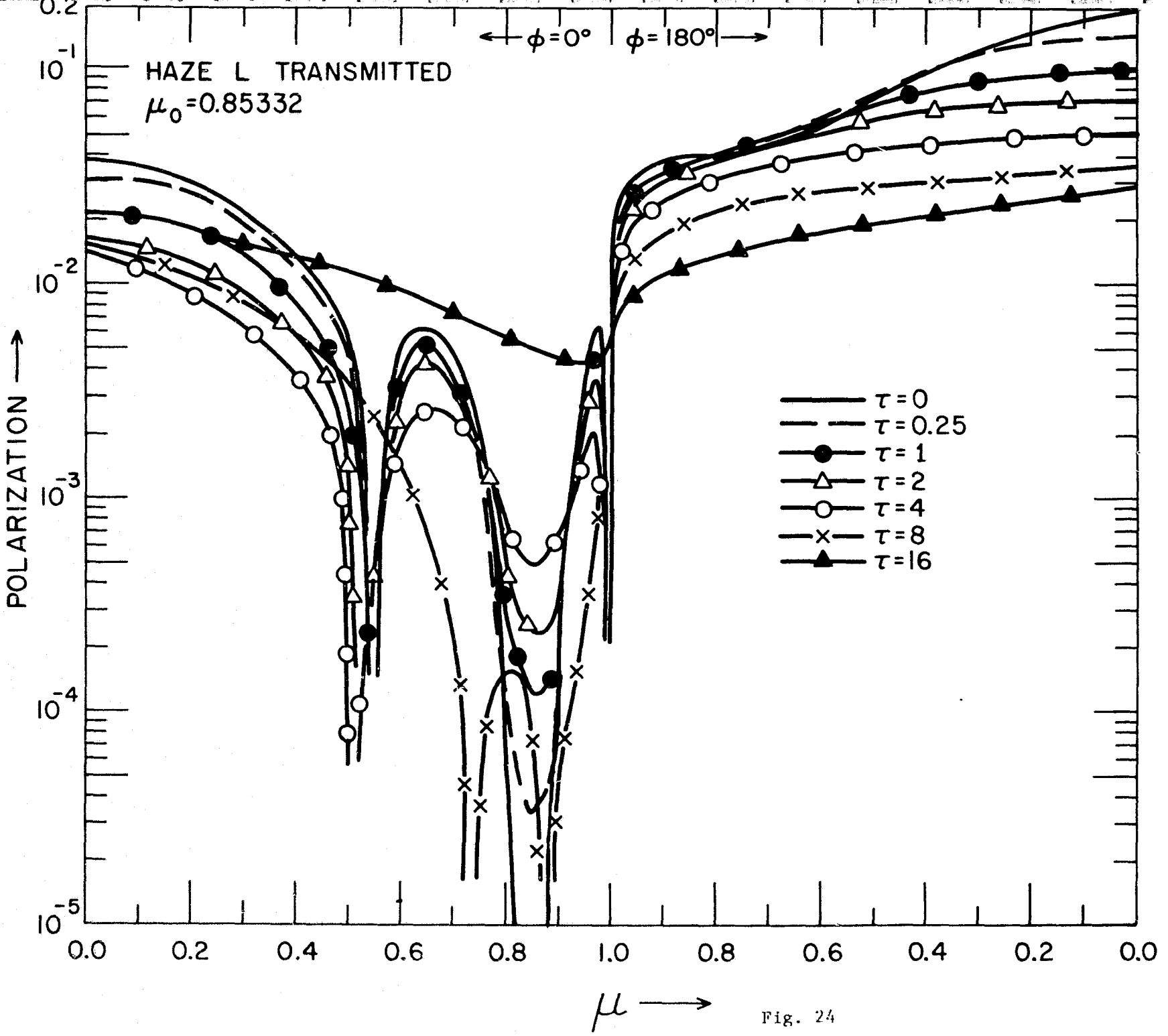
HAZE L TRANSMITTED
μ_0=0.85332
← ϕ=0° ϕ=180° →
POLARIZATION →
μ →
τ=0
τ=0.25
τ=1
τ=2
τ=4
τ=8
τ=16
0.2
10^{-1}
10^{-2}
10^{-3}
10^{-4}
10^{-5}
0.0
0.2
0.4
0.6
0.8
1.0
0.8
0.6
0.4
0.2
0.0

Fig. 24

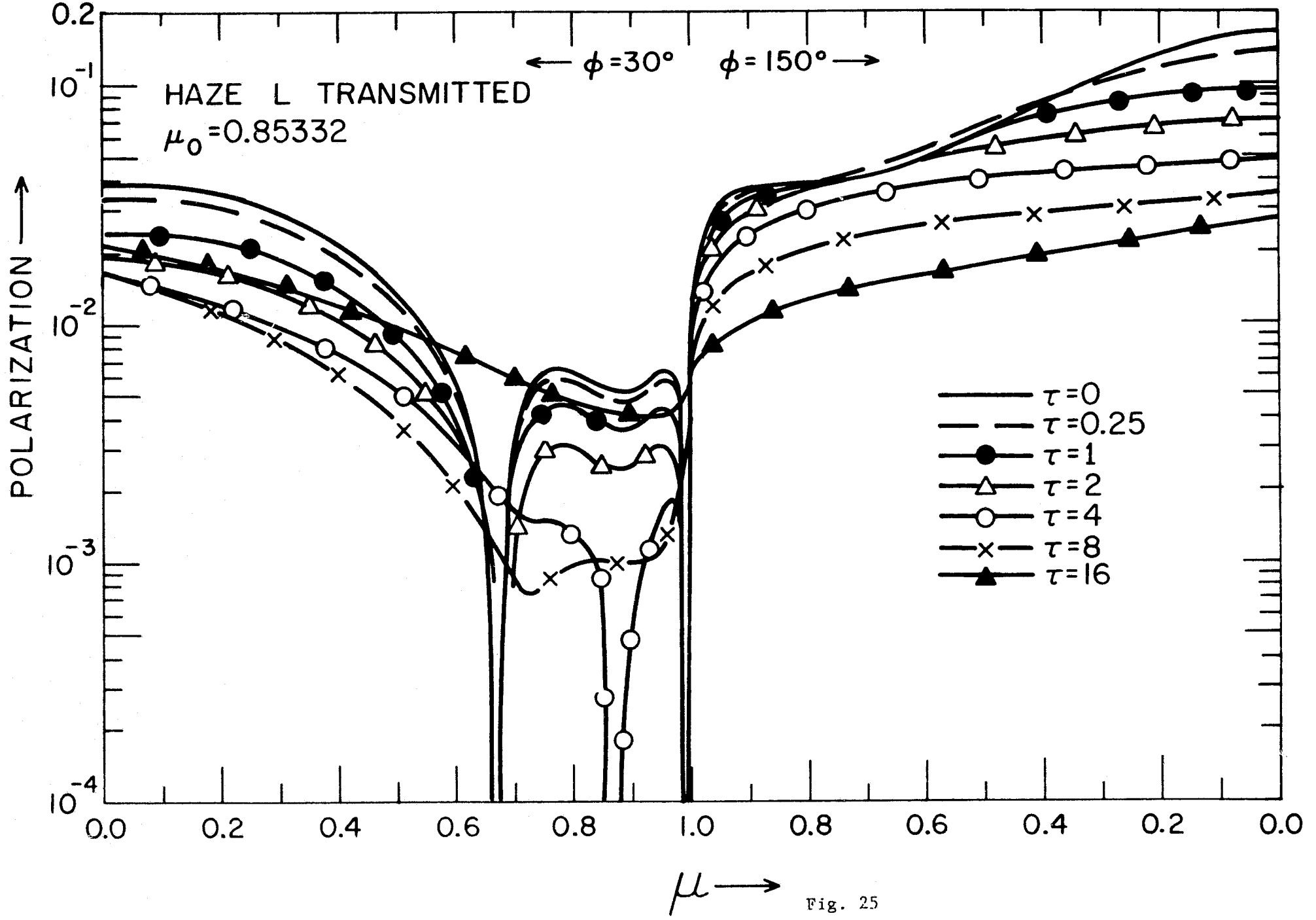
HAZE L TRANSMITTED
μ_0=0.85332
← ϕ=30° ϕ=150° →
POLARIZATION →
μ →
τ=0
τ=0.25
τ=1
τ=2
τ=4
τ=8
τ=16
0.2
10^{-1}
10^{-2}
10^{-3}
10^{-4}
0.0 0.2 0.4 0.6 0.8 1.0 0.8 0.6 0.4 0.2 0.0

Fig. 25

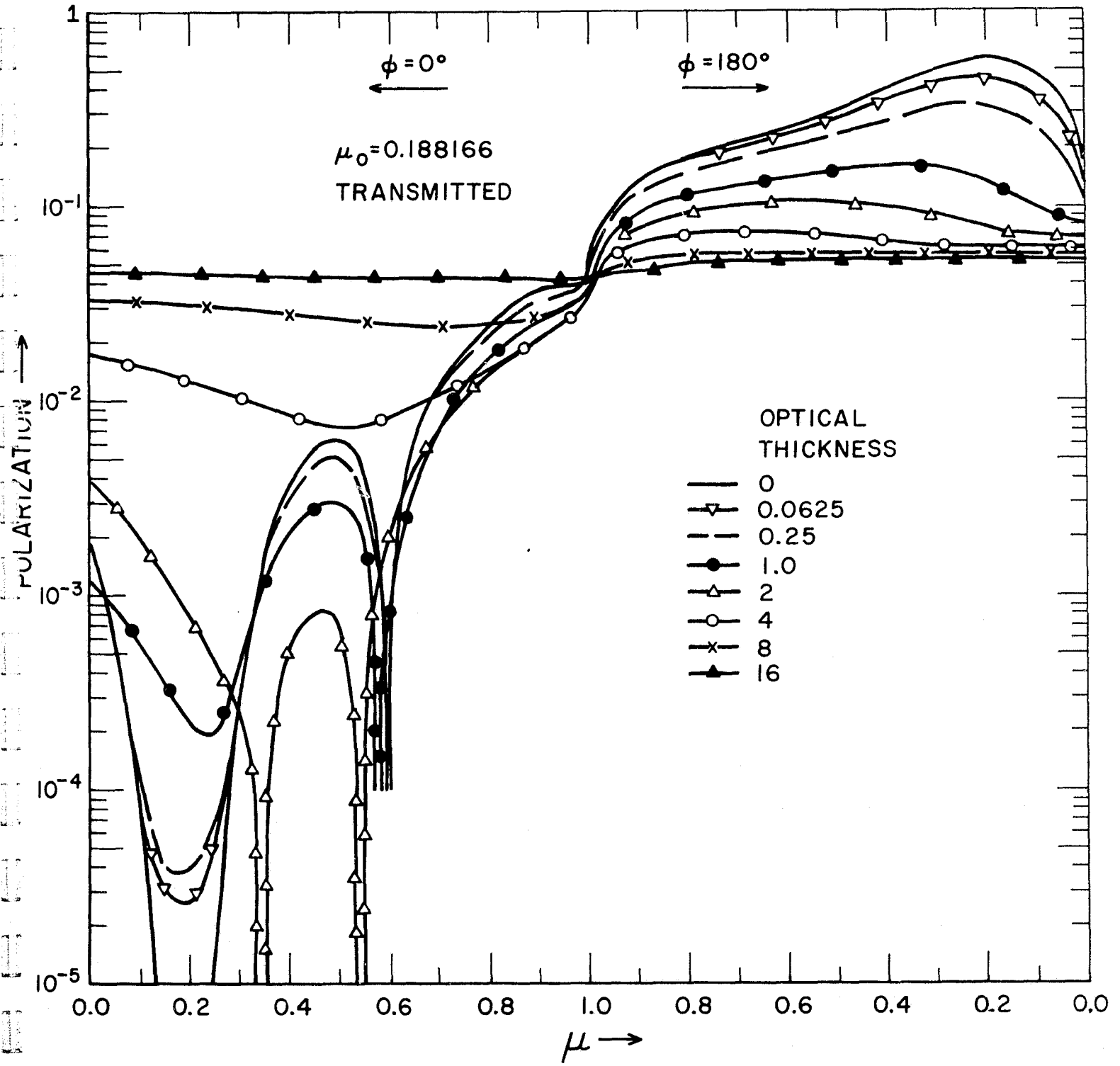
1
10^{-1}
10^{-2}
10^{-3}
10^{-4}
10^{-5}
POLARIZATION
$\phi = 0°$
$\phi = 180°$
$\mu_0 = 0.188166$
TRANSMITTED
OPTICAL THICKNESS
0
0.0625
0.25
1.0
2
4
8
16
0.0
0.2
0.4
0.6
0.8
1.0
0.8
0.6
0.4
0.2
0.0
μ

Fig. 26

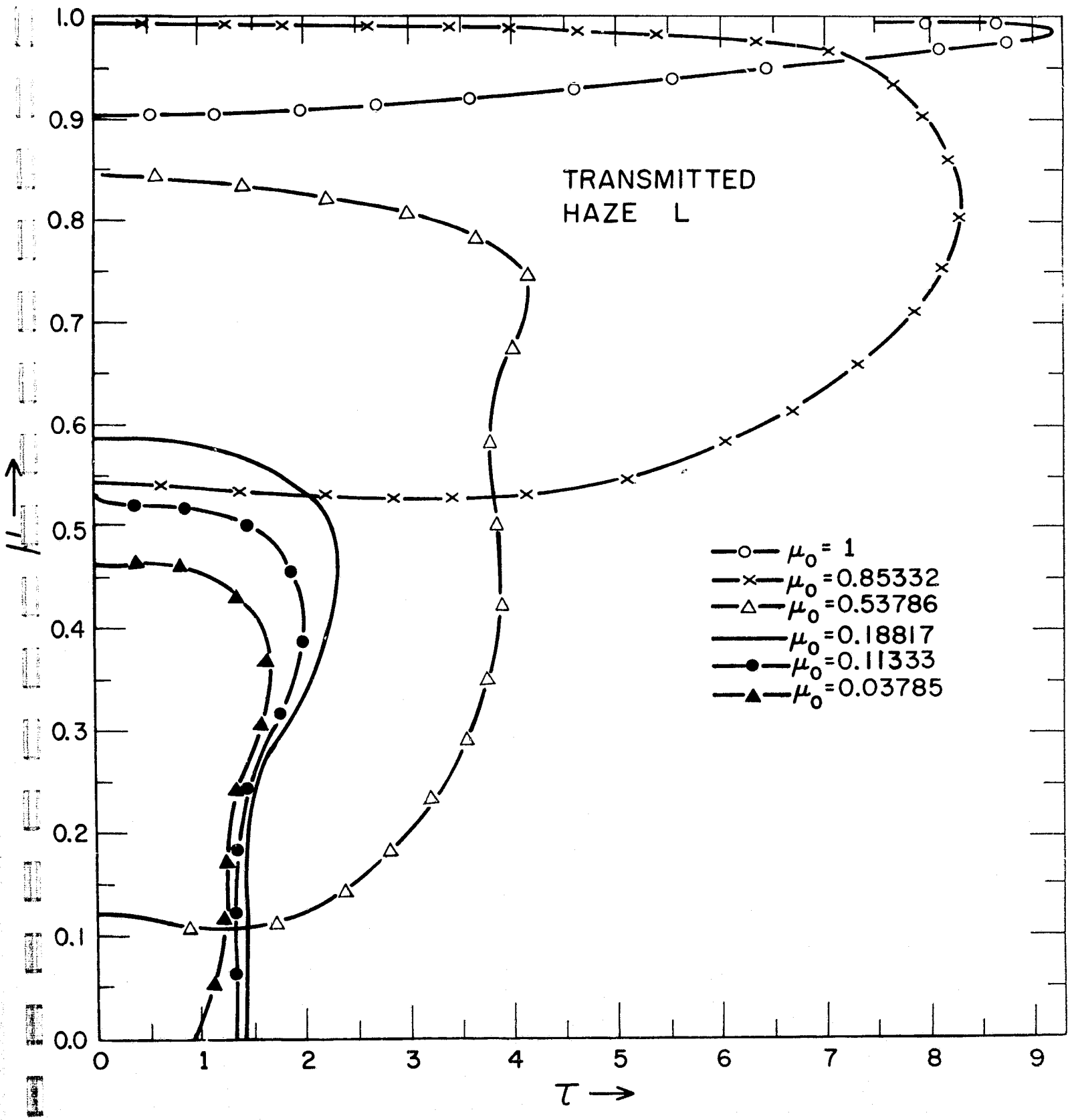
TRANSMITTED
HAZE L
$\mu_0 = 1$
$\mu_0 = 0.85332$
$\mu_0 = 0.53786$
$\mu_0 = 0.18817$
$\mu_0 = 0.11333$
$\mu_0 = 0.03785$
1.0
0.9
0.8
0.7
0.6
0.5
0.4
0.3
0.2
0.1
0.0
0
1
2
3
4
5
6
7
8
9
$\tau \rightarrow$

Fig. 27